Article

Probing sulfatide-tissue lectin recognition with functionalized glycodendrimersomes

SOLVING THE MYSTERY OF SULFATIDE FUNCTION

CLICKABLE BUILDING BLOCK AND GLYCODENDRIMERSOME SYNTHESIS

GLYCODENDRIMERSOME AGGREGATION WITH HETEROBIVALENT GALECTINS AND X-RAY CRYSTALLOGRAPHY

Paul V. Murphy,
Antonio Romero,
Qi Xiao, ...,
Michael L. Klein,
Virgil Percec,
Hans-Joachim
Gabius

paul.v.murphy@nuigalway.ie
(P.V.M.)
romero@cib.csic.es (A.R.)
juergen.kopitz@med.
uni-heidelberg.de (J.K.)
professorbovin@yandex.ru
(N.V.B.)
amwu@mail.cgu.edu.tw
(A.M.W.)
mlklein@temple.edu (M.L.K.)
percec@sas.upenn.edu (V.P.)
gabius@tiph.vetmed.
uni-muenchen.de (H.-J.G.)

HIGHLIGHTS

Nanoparticle
programming detects
sulfatide-(N)-glycan
bridging by galectins-4
and -8

Protein design (linker/
domain type) is a switch
for aggregation activity

Sphingosine's OH group
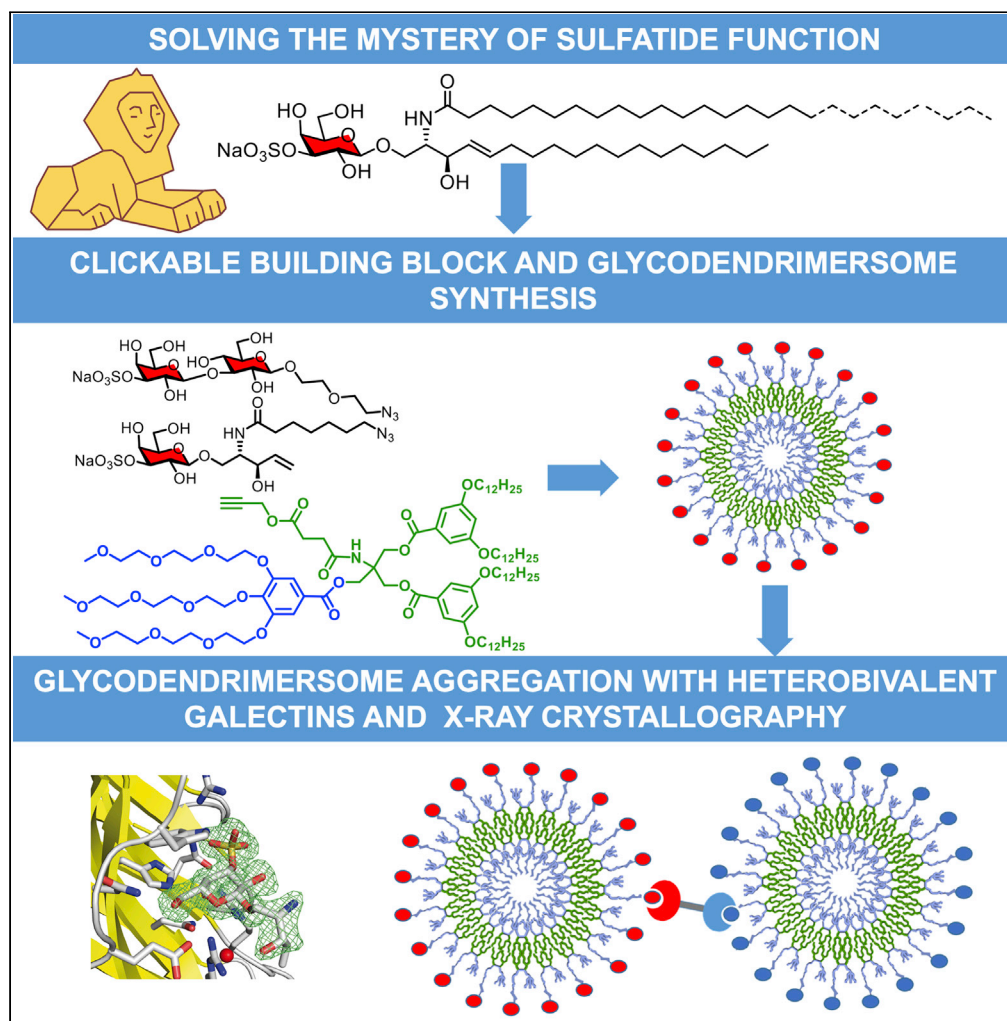is involved in contact
building with a galectin

CellPress
OPEN ACCESS

Article

Probing sulfatide-tissue lectin recognition with functionalized glycodendrimersomes

Paul V. Murphy,[1,10,11,*] Antonio Romero,[2,10,*] Qi Xiao,[3,4,10] Anna-Kristin Ludwig,[5,10] Srinivas Jogula,[1,10] Nadezhda V. Shilova,[6,7,10] Tanuja Singh,[8,10] Adele Gabba,[1] Bilal Javed,[4] Dapeng Zhang,[4] Francisco J. Medrano,[2] Herbert Kaltner,[5] Jürgen Kopitz,[9,*] Nicolai V. Bovin,[6,*] Albert M. Wu,[8,*] Michael L. Klein,[3,*] Virgil Percec,[4,*] and Hans-Joachim Gabius[5,*]

SUMMARY

The small 3-*O*-sulfated galactose head group of sulfatides, an abundant glycosphingolipid class, poses the (sphinx-like) riddle on involvement of glycan bridging by tissue lectins (sugar code). First, synthesis of head group derivatives for functionalization of amphiphilic dendrimers is performed. Aggregation of resulting (biomimetic) vesicles, alone or in combination with lactose, demonstrates bridging by a tissue lectin (galectin-4). Physiologically, this can stabilize glycolipid-rich microdomains (rafts) and associate sulfatide-rich regions with specific glycoproteins. Further testing documents importance of heterobivalency and linker length. Structurally, sulfatide recognition by galectin-8 is shown to involve sphingosine's OH group as substitute for the 3′-hydroxyl of glucose of lactose. These discoveries underscore functionality of this small determinant on biomembranes intracellularly and on the cell surface. Moreover, they provide a role model to examine counterreceptor capacity of more complex glycans of glycosphingolipids and to start their bottom-up glycotope surface programming.

INTRODUCTION

The "many enigmas" around a major component of "alkaloidal nature" in ethanolic brain extracts, i.e. sphingosine, and the sphingolipids are symbolized by their names: they originate from the sphinx and its famous riddle (Sourkes, 2003; Thudichum, 1884). Thudichum's detection of neutral sugar in phrenosine, now called galactocerebrosides, and its 3-*O*-sulfated derivative in sulfatides has started efforts to explain the abundant presence of a lipid-linked monosaccharide and its site-specific sulfation. Of course, it is reasonable to assume that these simple compounds are more than inert constituents of the lipid bilayer (Ishizuka, 1997; Takahashi and Suzuki, 2012; Vos et al., 1994; Yamakawa et al., 1962). As an attractive possibility, the concept of the sugar code considers the glycan part of glycosphingolipids as a biochemical message anchored in the membrane, and thereby presented on its surface ready for being 'read' by receptors (Gabius and Roth, 2017; Kaltner et al., 2019). Herein, we focus on the head group of sulfatides, whose enzymatic synthesis is made possible by (galactosyl)cerebroside 3-*O*-sulfotransferase (CST, Gal3ST-1). The occurrence of further sulfotransferases acting on sugars and their diversification to gain selectivity for diverse substrates are the pillars of the hypothesis for (patho)physiological relevance of glycan sulfation, which is assumed to convert rather small glycans (even a monosaccharide) into potent ligands (Bowman and Bertozzi, 1999; Fukuda et al., 2001; Hemmerich and Rosen, 2000; Hooper et al., 1997).

With respect to 3-*O*-sulfation of galactose, more than one enzyme with this activity has evolved. In addition to sulfatide generation, galactose of *N*-acetyllactosamine (LacNAc) at branch ends of glycan chains after protein glycosylation is a substrate (for Gal-3ST-2/-3; products shown in Figure 1) (Fukuda et al., 2001). In comparison to the advanced status of the characterization of the enzymatic machinery for the 3-*O*-sulfation of galactose, precise elucidation of the actual profile of bioactivities of the products as ligand lags behind. Respective efforts would benefit from a testing with a chemically prepared sulfatide analog and a fully programmable model system, tailored to be in principle useful for any type of glycosphingolipid ensuring broad-scale applicability. It is a challenge for synthetic and supramolecular chemistry to create the respective toolbox to put the assumption of involvement of the sulfatide head group in cross-linking processes by tissue receptors to the test.

[1]CÚRAM – SFI Research Centre for Medical Devices and the School of Chemistry, National University of Ireland Galway, University Road, Galway H91 TK33, Ireland

[2]Department of Structural and Chemical Biology, CIB Margarita Salas, CSIC, Ramiro de Maeztu, 9, 28040 Madrid, Spain

[3]Institute of Computational Molecular Science, Temple University, Philadelphia, PA 19122, USA

[4]Roy & Diana Vagelos Laboratories, Department of Chemistry, University of Pennsylvania, Philadelphia, PA 19104-6323, USA

[5]Institute of Physiological Chemistry, Faculty of Veterinary Medicine, Ludwig-Maximilians-University Munich, Veterinärstr. 13, 80539 Munich, Germany

[6]Shemyakin & Ovchinnikov Institute of Bioorganic Chemistry, Russian Academy of Sciences, 16/10 Miklukho-Maklaya str., 117437 Moscow, Russian Federation

[7]National Medical Research Center for Obstetrics, Gynecology and Perinatology named after Academician V.I. Kulakov of the Ministry of Healthcare of Russian Federation, 4 Oparina str, 117997 Moscow, Russian Federation

[8]Glyco-Immunology Research Laboratory, Institute of Molecular and Cellular Biology, Chang-Gung-Medical College, Kwei-san, Tao-yuan 333, Taiwan

[9]Zentrum Pathologie, Institut für Angewandte Tumorbiologie, Medizinische Fakultät der
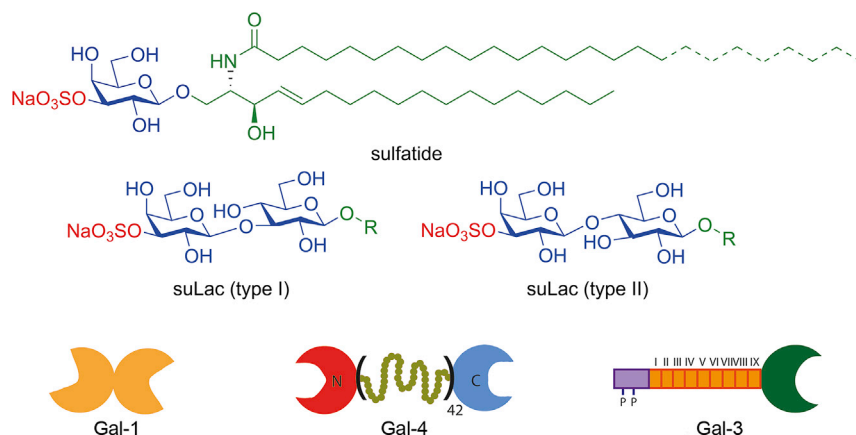
Continued

Figure 1. The toolbox of our study
The carbohydrate ligands and the three forms of architecture of human galectins, i.e. non-covalently associated homodimer, linker-connected heterodimer (galectin-4 [Gal-4] with a 42 amino-acid-long linker) and lectin domain with N-terminal tail containing collagen-like repeats and a peptide with two sites of serine phosphorylation.

Like the glycosphingolipids, known endogenous receptors for their glycan part (lectins) present their own mysteries (Ledeen et al., 2018). Especially the occurrence of diverse types of modular architecture is not yet fully understood in functional terms. As illustrated in the bottom part of Figure 1 for vertebrate galectins, three distinct forms are found (García Caballero et al., 2020; Kaltner et al., 2017). Concerning sulfatides as ligands, binding has up to now been reported for human galectins-4 and -8 (Gal-4 and -8) using the glycosphingolipid adsorbed to a plastic surface, the interaction with Gal-4 on the cellular level implicated in stabilization of enterocyte membrane microdomains rich in (glyco)lipids and -proteins (lipid rafts, also known as a fundamental platform for starting outside-in signaling) and in sulfatide-dependent apical/axonal routing of distinct glycoprotein cargo (likely predestined for recognition by a high density of LacNAc of complex-type N-glycans) (Braccia et al., 2003; Danielsen and van Deurs, 1997; Delacour et al., 2005; Ideo et al., 2003; 2005; Morelle et al., 2009; Stechly et al., 2009; Velasco et al., 2013). However, a physical bridging required for these processes has not yet been demonstrated. As shown by array testing with glycans and by galectin-dependent cell association of neoglycoconjugates (Blixt et al., 2004; Vokhmyanina et al., 2012), as well as by cocrystallization of both CRDs of Gal-4 with oligosaccharides (Bum-Erdene et al., 2015, 2016), the apparent dual specificity of Gal-4 to neutral and to sulfated glycans will have an obvious consequence for attempts to show functional bivalency and bridging: it requires to take assay and nanoparticle designs from a single defined epitope to mixed systems, hereby establishing the starting point for bottom-up tailoring to eventually reproduce cellular biodiversity. In detail for this context, the components for assays are built to simulate the natural presentation of substituted (sulfatide) and unsubstituted (glycoprotein) β-galactosides; this way, chemical proof-of-principle tools for examining the possibility of an actual realization of dual specificity of Gal-4 *in vivo* are established.

Here, we describe preparation of conjugatable headgroups and their alkyne-functionalized adapter for linking sulfatide derivatives to a lipid anchor to prepare custom-made amphiphilic Janus glycodendrimersomes (GDSs), which made galectin testing (incl. architecture variants obtained by protein engineering) possible: this strategic combination is applied as a step to solve pertinent mysteries both on (ga)lectin/glycosphingolipid presence and on structural diversity of galectins. The advantage of proof-of-principle work with amphiphilic Janus glycodendrimers, besides the perspective for chemical programming of the nanoparticle surface, is gaining access to diverse morphologies relevant for pathobiology such as cubosomes (Xiao et al., 2016a) or for galectin secretion, that is onion (multivesicular body)-like GDSs (Xiao et al., 2016b). Of course, application of synthetic glycodendrimers in classical systems such as liposomes will also be possible.

After having described the procedures to obtain the suited conjugatable head group derivatives and to nanoparticles as well as after having detected and mapped their activity profile in *trans*-interactions by aggregation assays, we also probed into the structural basis of contact building on the atomic level. This process commonly requires extension of galactose to the disaccharide (lactose) for galectins so that the

Ruprecht-Karls-Universität Heidelberg, Im Neuenheimer Feld 224, 69120 Heidelberg, Germany

[10]These authors contributed equally

[11]Lead contact

*Correspondence:
paul.v.murphy@nuigalway.ie (P.V.M.),
romero@cib.csic.es (A.R.),
juergen.kopitz@med.uni-heidelberg.de (J.K.),
professorbovin@yandex.ru (N.V.B.),
amwu@mail.cgu.edu.tw (A.M.W.),
mlklein@temple.edu (M.L.K.),
percec@sas.upenn.edu (V.P.),
gabius@tiph.vetmed.uni-muenchen.de (H.-J.G.)

https://doi.org/10.1016/j.isci.2020.101919
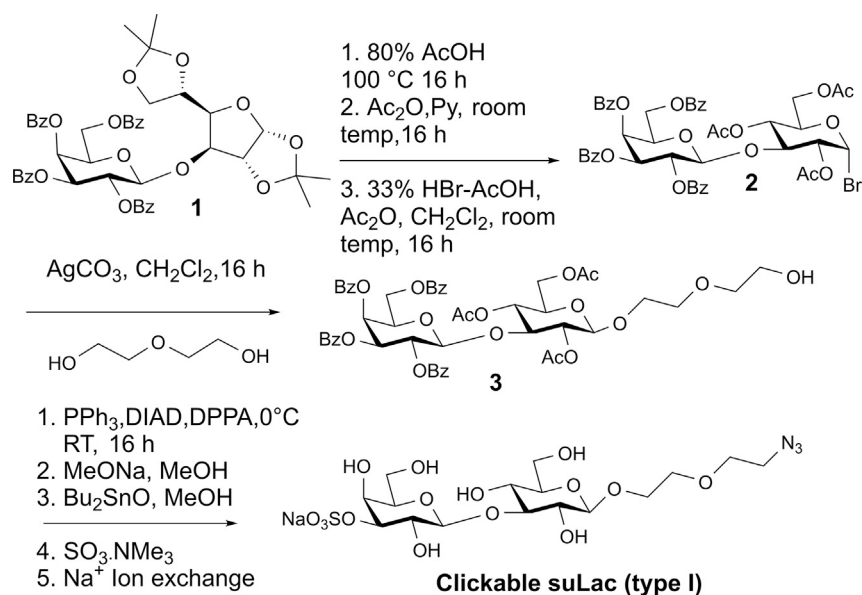
Scheme 1. Synthetic route to the clickable suLac (type I) derivative
See also Figure S3.

glucose moiety can contribute, as revealed for the galectin CRD by crystallography (Kamitori, 2018; Romero and Gabius, 2019) and by chemical mapping (Solís et al., 1996). The data obtained by crystallography with the synthetic head group are first evidence that a non-glycan determinant, here sphingosine's hydroxyl group, is involved in sulfatide pairing with a galectin via water-mediated contacts, as the 3-OH group of glucose of the canonical ligand lactose otherwise does by direct hydrogen bonding.

RESULTS AND DISCUSSION
Sulfated lactose as ligand

As a step to elucidate ligand properties of sulfated galactose comparatively, we first prepared *O*-sulfated galactose in β1,3-linkage to glucose (termed suLac (type I)). Its synthesis starting from galactopyranoside **1** (Crich et al., 2005) is summarized in Scheme 1.

The attachment of the azide-bearing glycan derivative to the lipid anchor alkyne by click chemistry (Percec et al., 2013; Zhang et al., 2014) and the resulting product shown in Figure S1 (left) self-assembled into GDSs (D_{DLS} = 64 nm, PDI = 0.27). Their application in aggregation assays documented that both CRDs in the heterobivalent Gal-4 can associate to this type of ligand, hereby bridging the suLac (type I)-bearing GDSs (Figure 1). A single CRD or a CRD mixture is unable to connect particles, highlighting the need for integrity of the linker. Endpoint determination indicates a reduced OD value relative to testing suLac (type II) (Xiao et al., 2018). In order to examine the importance of the nature of the linker between the two CRDs in this galectin architecture, we produced variants with shortened sequence or without such extension. Intriguingly, not length reduction (see Gal-4V with 16 amino acids instead of 42 amino acids in the linker in Figure 1, bottom center) but the complete removal of the linker between the CRDs by cDNA engineering visibly decreased extent of aggregation (see Gal-4P in Figure S1). Since profiles of array binding appear influenced by the nature of the CRD and also the length of the linker (Figure S2), the results of these assays inform us about notable consequences of reduction of the length of the linker. Since proto-type galectins form homodimers by non-covalent association, their testing will answer the question on differences in bridging capacity.

Interestingly, homodimeric (linker-free) Gal-1, -2 and -7 are active, pointing to a combination of nature of CRD and architecture of its presentation for extent of activity (Figure S1, right). The relative signal intensities for Gal-1 and -8 were similar, as independently reported from using AlphaScreen technology (Tu et al., 2013). Equally important, the chimera-type Gal-3 (Figure 1, bottom-right; monomeric in solution) becomes an aggregant for this ligand, whereas Lac presentation is not sufficient to trigger bridging capacity
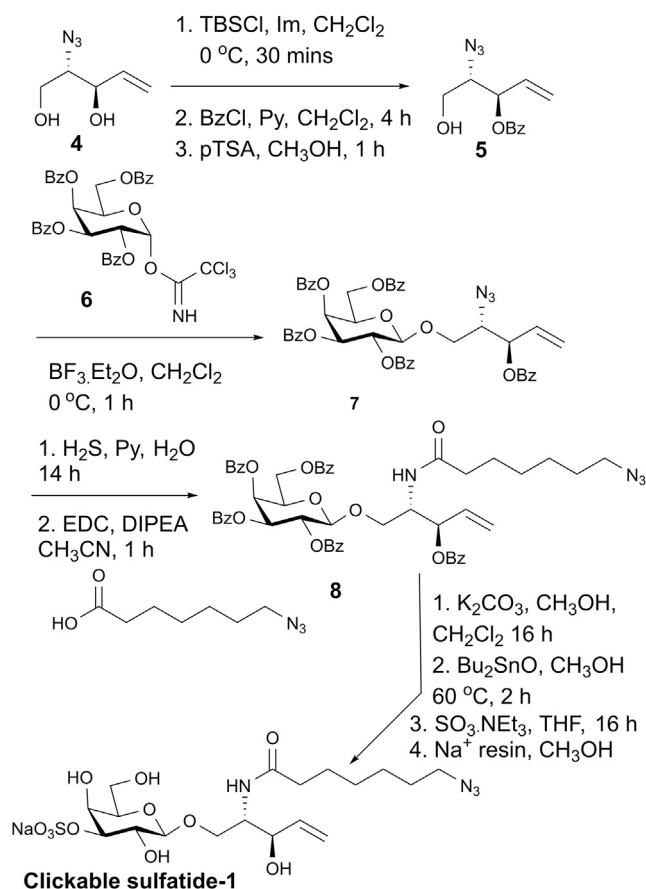
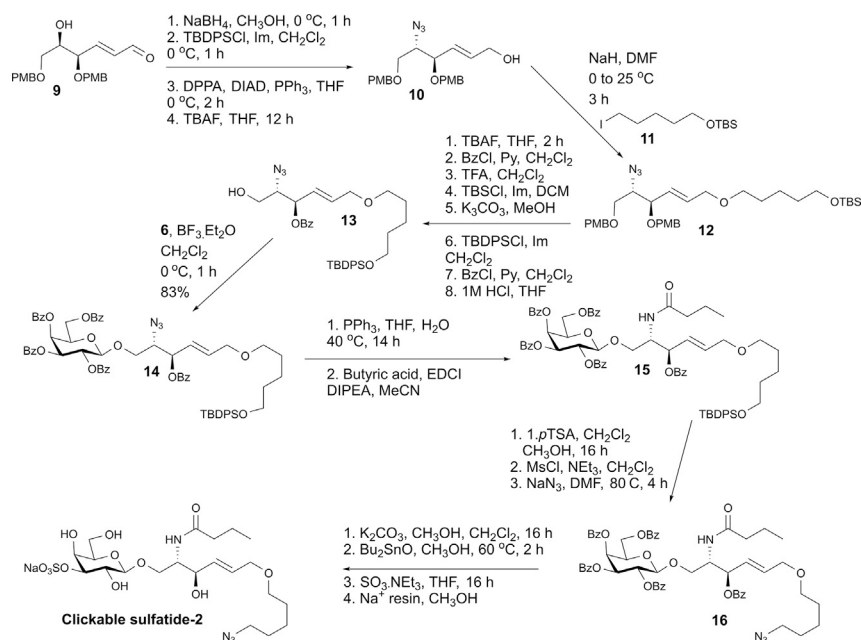**Scheme 2. Synthetic route to the clickable sulfatide-1 derivative**
See also Figure S3.

(Figure S1, right). 3-*O*-sulfated galactose presented by Lac thus is a galectin ligand, tuning of activity occurs by the linker for Gal-4. This documented, we can next address the open question whether cross-linking of ligands on opposing surfaces can still occur after shortening the canonical ligand Lac to the monosaccharide as is the case in sulfatides: only then could Gal-4 bring sulfatides on neighboring rafts as well as sulfatide (preferentially with C24 acyl chain) in such microdomains and glycoprotein cargo with LacNAc (or suLac) termini together physiologically.

The sulfatide head group as ligand

The structure of the sulfatide hinge region to the acyls (Figure 1, top) suggests two sites for placement of the azide, i.e. in the palmitoyl CoA-derived acyl or in the second acyl (physiologically of variable length, which explains diversity for sulfatides; a C24 chain ensures accessibility). Each of the two routes was taken. The diol **4** described in a patent by (Bundle et al., 2003) with an additional azide group was converted to sulfatide-1 by the steps given in Scheme 2.

Alternatively, the clickable azide was introduced into the core structure at the second acyl by the pathway from **9** summarized in Scheme 3.

The two products were connected to the standard lipid anchor to set the stage for their self-assembly (Figure S3). The GDSs subsequently prepared, using either sulfatide-1 (D_{DLS} = 108 nm; PDI = 0.18) or sulfatide-2 (D_{DLS} = 147 nm; PDI = 0.27) (Figure 2, bottom-left), present a surface mimicking (*cum grano salis*) sulfatide presence in detergent-resistant membrane sections. Remarkably, these artificial nanoparticles established the assay platform to explore sulfatide activity as ligand in our study. Compared with suLac (type I), their ligand activity for Gal-4 was rather small but clearly detectable (Figure 2). The previously reported occurrence of

Scheme 3. Synthetic route to the clickable sulfatide-2 derivative
See also Figure S3.

"superrafts" heavily enriched in galectin-4 in microvillar membranes of pig small intestine (Braccia et al., 2003) could thus originate from sulfatide-Gal-4 cross-linking in regions of mutually high density.

Since Gal-4 had also been implicated in arranging glycoprotein segregation by *trans*-interactions, that is to bridge sulfatide and LacNAc of clustered *N*-glycans of distinct glycoproteins, then extent of galectin-dependent aggregation in mixed systems (a GDS mixture or GDSs obtained from two glycodendrimers mixed at different ratio) will be a respective sensor. The inert sugar mannose (Man) serves as negative control (Figure 3A). The illustrated baseline OD_{450}-reading excludes a cognate-carbohydrate-independent aggregation, a general stickiness of ethylene glycol being the concern. The experience with glycoclusters containing similar linker structures, e.g. reported by (André et al., 2009, 2010), with a PEGylated galectin that does not self-associate, even exerting repulsion (He et al., 2010) and with other types of galectins and sugars of graded interaction potential (Ludwig et al., 2019a; Zhang et al., 2015) builds a solid body of evidence against such unwanted side effects. Moreover, a contact site found for glycerol in the N-terminal domain of murine Gal-4 is spatially distinct from the surface pocket binding lactose (Krejciríková et al., 2011), allowing them to distinguish bindings by competitive inhibition.

Figure 3 presents evidence for increased extent of aggregation of nanoparticle mixtures for the pair of Gal-4 and sulfatide-1-bearing GDSs (top). Presence of the sulfatide head groups increased the threshold for aggregation relative to Man when testing GDSs obtained from glycodendrimer mixtures (Figure 3, top). Physiologically, the density of LacNAc termini on *N*-glycans of a glycoprotein can thus be a criterion for counterreceptor selection, what has actually been suggested (Morelle et al., 2009). The data of our panel testing of glycoproteins (Tables S1 and S2, and Figure S4) support this concept.

Having revealed physical contacts in this heterotypic (pseudophysiological) system, the question can be addressed next as to whether Gal-4 is unique for this interplay. Respective testing disclosed aggregation also for Gal-8 (Figure 3, bottom, left). Wild-type Gal-3 that effectively connects suLac head groups (see above) fails to do the same with sulfatide. Of particular note, the Gal-3 CRD yet becomes an active cross-linker after its engineering to a homodimer with a linker (Figure 3, bottom row): obviously, the protein design is crucial and its alteration by engineering is like a molecular switch. Homodimeric Gal-1, in contrast, shows no evidence for a bridging activity of sulfatide headgroups (Figure S5). The loss of contact to the Glc(NAc) part of suLac(NAc) may play a significant role here, when noting the respective capacity of suLac as docking point. The two tandem-repeat-type galectins thus appear to use a compensatory contact for
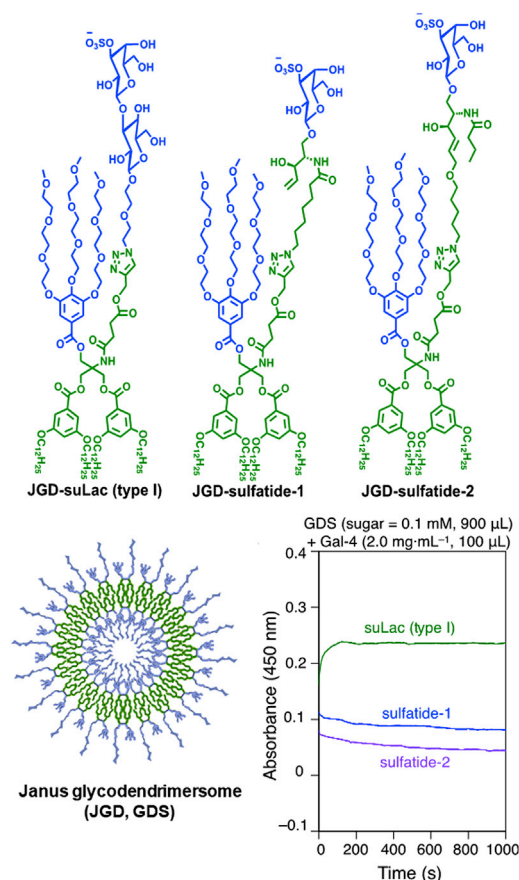
Figure 2. Glycodendrimer and Janus GDS structures (top, bottom-left) and course of aggregation of GDSs by Gal-4 in PBS (pH = 7.4) (bottom-right)
See also Figure S3.

acquiring stability, and here sphingosine's hydroxyl group comes into play as a possibility. A means to test the validity of this hypothesis is crystallographic study, if a complex of a galectin CRD with synthetic sulfatide-1 could be obtained.

Crystallography of Gal-8N with a sulfatide head group

Systematic testing of conditions with the N-terminal CRDs of Gal-4 and -8 led to crystals for Gal-8N and thus data to decide the issue (Figure 4, Table S3, PDB: 6Z6Y). Clear electron density for the head group structure was obtained, whereas the amide's acyl chain appeared rather mobile, so that a profiling of the head group's contacts became possible. As depicted in Figure 4A on two levels of magnification, the galactose moiety with its sulfate was central to contact building. This was expectable, when considering the analogy to cocrystals of this CRD with lactose and 3'-sialyl- and 3'-sulfolactose ligands (Ideo et al., 2011). In this position, sphingosine's hydroxyl group and side chains of Arg69/Glu89, together with a water molecule, are connected by hydrogen bonding. It hereby appears to functionally substitute the 3'-hydroxyl group of the glucose part of lactose (Figure 4B). The intriguing structural equivalence of sphingosine's hydroxyl group with the 3'-hydroxyl group of glucose of suLac, shown in Figure 4C (PDB: 3AP6), is illustrated in Figure 4D, with the water-mediated network taking the place of the direct hydrogen bonding. When using a suLac-Gal-4N structure as platform (PDB: 5DUW, Figure 4E) and arranging key contacts for galactose and sulfate accordingly, a similar structural equivalence is seen (Figure 4F).

Conclusions

The synthesis of two forms of clickable sulfatide head group has facilitated the generation of GDSs with biomimetic model character for glycosphingolipids. This platform offers the perspectives to further modify
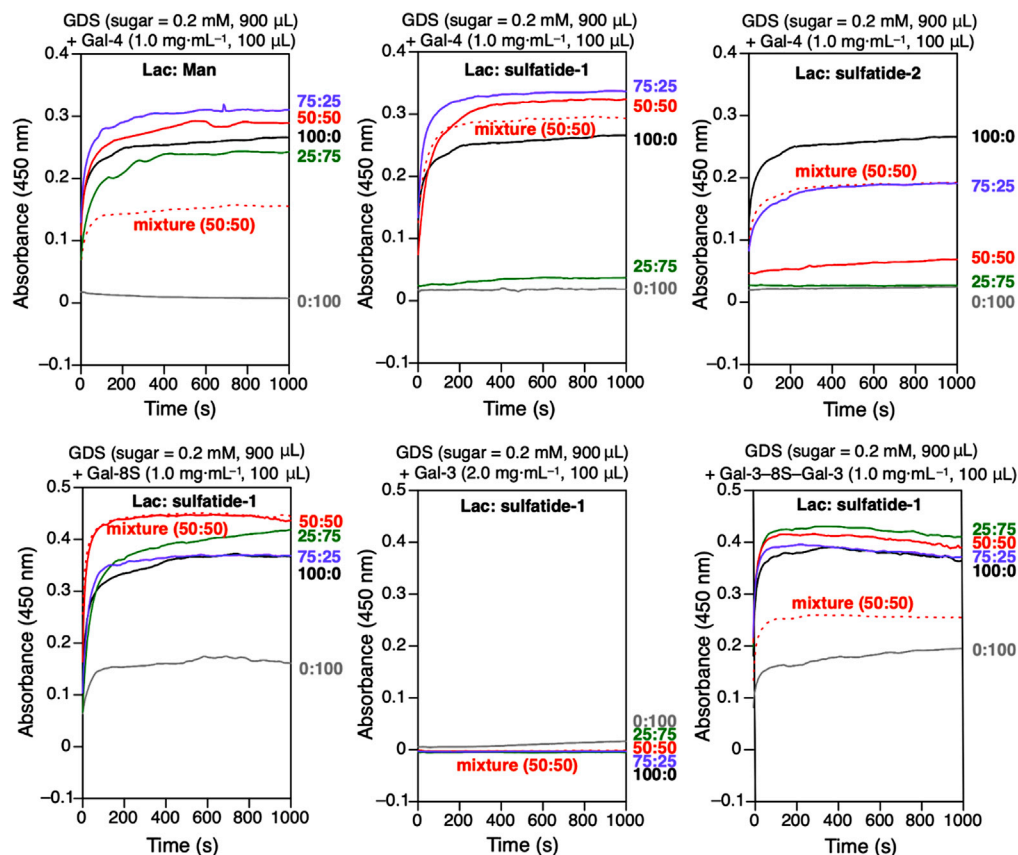
Figure 3. Galectin- and glycan-dependent bridging of GDSs
Course of aggregation of co-assembled GDSs by Gal-4, Gal-8S, Gal-3, and the linker-connected homodimeric Gal-3 variant (termed Gal-3-8S-Gal-3) in PBS (pH = 7.4). (See also Figure S3).

their surface presentation by additions of other membrane constituents such as cholesterol (Róg and Vattulainen, 2014) and to build a library of test tools including typical glycans of glycoproteins. Starting with sulfated lactose, it is shown to be a docking point for human galectins. This contact enables bridging irrespective of their architecture, even in the case of wild-type Gal-3. Presentation of the sulfatide head group yielded a rather weak but significant aggregation activity for Gal-4 in the homotypic system. This interaction can physiologically underlie reported raft stabilization and superraft formation. In GDSs mixtures simulating sulfatide and glycoprotein presence, the sulfatide-1 structure supported aggregation: this can mimic recruitment of glycoprotein cargo to heterobivalent Gal-4 presented by its association to sulfatide in detergent-resistant membranes. Bringing together two different CRDs that share binding to sulfatide and have context-dependent preferences, as indicated also by galectin histochemistry with fusion proteins of the CRDs (Wasano and Hirakawa, 1999), makes this functional versatility possible. As GDSs as sensor for contact building disclose, the presence of the linker is important for accepting clustered glycan arrangements as binding site, ligand binding to Gal-4 in solution then yielding a rather compact structure favoring cargo transport (André et al., 2014; Göhler et al., 2010).

In structural terms intriguing, sphingosine's OH group can be involved in galectin-sulfatide interaction, as shown by crystallography. The importance of the illustrated physical contact of sulfatide with sugar and sphingosine is underscored by pointing to likely physiological back-ups: in the absence of sulfatide, cholesterol 3-sulfate may well play this role (Ideo et al., 2007), and our data suggest that Gal-8 is a candidate to compensate for a genetic deficiency in Gal-4 expression, this possibility discussed in principle for a Gal-3 animal model (Eude-Le Parco et al., 2009). Since homodimeric Gal-1 is not a sulfatide receptor and chimera-type Gal-3 is only converted into a receptor by an engineered change of architecture, perspectives of further strategic combinations of this type of supramolecular tool with generation of innovative protein design (lectinology 4.0 (Ludwig et al., 2019b)) are obvious.
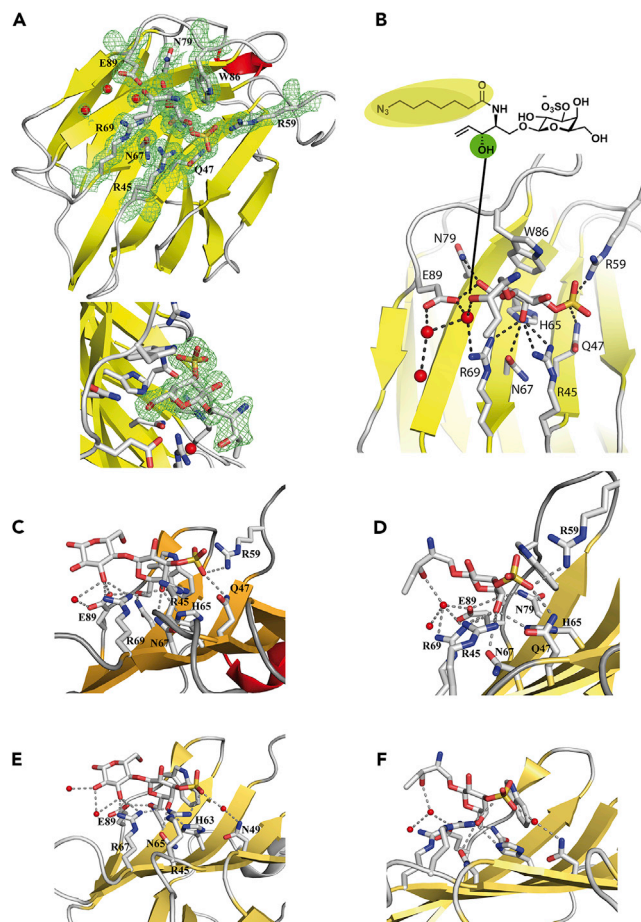
Figure 4. Structural equivalence of hydroxyl groups of glucose/sphingosine

(A–F) (A) Relevant section of Gal-8N complexed with the sulfatide-1 as 2Fo-Fc electron density map contoured at 1.0 σ (protein drawn in cartoon-style, sulfatide-1 and contact residues in ball-and-stick mode and water molecules red spheres) at two levels of magnification and (B) profile of interactions, highlighting sphingosine's OH group and the mobile acyl section of the amide. Comparative illustration of the relevant sections of Gal-8N-ligand complexes for suLac (PDB: 3AP6; C) and for sulfatide-1 (D) showing the structural equivalence of the hydroxyl groups of sugar (C) and sphingosine (D). This is also seen for Gal-4N-ligand complexes, i.e. Gal-4-N with suLac (PDB: 5DUW); (E) and the correspondingly modeled complex with sulfatide-1 (F).

Finally, the reported homo- and heterobivalency in the cross-linking assays explains well a role of Gal-4 in detergent-resistant membranes, and it may also underlie its specific role as suppressor for human colon cancer (Michalak et al., 2017, 2019; Rao and Rao, 2017; Rechreche et al., 1997; Satelli et al., 2011), as factor in oligodendrocyte differentiation and as inhibitor of myelination (de Jong et al., 2018, 2020; Díez-Revuelta et al., 2017; Stancic et al., 2012). Thus, the applied synthetic and supramolecular chemistry that led to detection of GDS bridging by sulfatide-Gal-4 pairing identifies a versatile means of letting sulfatide presence appear less enigmatic. This conclusion encourages further studies with the GDS platform on other sulfatide-binding proteins, i.e. adhesive glycoproteins laminin or thrombospondin (Roberts and Ginsburg, 1988), L-selectin (Honke et al., 2004; Suzuki et al., 1993), and Ig-like receptor LMIR5 (Phongsisay et al., 2015), intracellularly the HIF-1 target NOD2 (Nabatov et al., 2013), and on carbohydrate-carbohydrate interactions (Bovin, 1997; Zhao et al., 2012).

Limitations of the study

The documented attractive possibility for versatile surface programming should not lead to take the analogy to a biorelevant design too far. Typical segregation into microdomains known from cellular membranes can not yet be mimicked. Mixtures with natural (glyco)sphingolipids and glycerophosphatides

typically bearing unsaturated acyl chains and addition of cholesterol are then helpful to constitute systems with a larger number of variables that can implement and regulate fluidity. Variation of acyl chain length, for example to the C24 form of sulfatide assumed to be the preferential binding partner (Delacour et al., 2005), is likely to have an impact, too, as incorporation of such artificial glycolipids, which are obtained by the described head group synthesis and conjugation to an anchor, into liposomal or even cellular membranes can be envisioned, all with the aim to come as close to the biochemical and spatial heterogeneity of a natural membrane as possible. Equally important, the monitoring of OD_{450}-value changes upon aggregation is the starting point for quantitative analysis of galectin binding including quantifying *cis*-interactions and the strength of cohesion. Nonetheless, this platform teamed up with head group tailoring and protein engineering affords a robust system to detect bridging activity of physiological relevance, as shown here by the introduction of the heterotypic aggregation assay and a human lectin actually involved in apical transport.

Resource availability

Lead contact

Further information and requests for resources should be directed to and will be fulfilled by the Lead contact, Paul V. Murphy (paul.v.murphy@nuigalway.ie).

Materials availability

This study did not generate new unique reagents.

Data and code availability

The published article includes all datasets/code generated or analyzed during this study.

METHODS

All methods can be found in the accompanying Transparent Methods supplemental file.

SUPPLEMENTAL INFORMATION

Supplemental Information can be found online at https://doi.org/10.1016/j.isci.2020.101919.

AUTHOR CONTRIBUTIONS

Conceptualization, P.V.M. and H.-J.G; Methodology, P.V.M., A.-K.L., H.K., N.V.B., A.M.W., M.L.K., and V.P.; Investigation, A.R., Q.X., S.J., N.V.S., T.S., A.G., B.J., D.Z., and F.J.M.; Writing-Original Draft: P.V.M., A.R., J.K., M.L.K., and H.-J.G.; Writing-Review & Editing, P.V.M., A.R., and H.-J.G.; Supervision, P.V.M., and H.-J.G.; Project Administration, P.V.M., and H.-J.G.

DECLARATION OF INTERESTS

The authors declare no competing interests.

REFERENCES

André, S., Specker, D., Bovin, N.V., Lensch, M., Kaltner, H., Gabius, H.-J., and Wittmann, V. (2009). Carbamate-linked lactose: design of clusters and evidence for selectivity to block binding of human lectins to (neo)glycoproteins with increasing degree of branching and to tumor cells. Bioconj. Chem. 20, 1716–1728.

André, S., Lahmann, M., Gabius, H.-J., and Oscarson, S. (2010). Glycocluster design for improved avidity and selectivity in blocking human lectin/plant toxin binding to glycoproteins and cells. Mol. Pharmaceut. 7, 2270–2279.

André, S., Wang, G.N., Gabius, H.-J., and Murphy, P.V. (2014). Combining glycocluster synthesis with protein engineering: an approach to probe into the significance of linker length in a tandem-repeat-type lectin (galectin-4). Carbohydr. Res. 389, 25–38.

Blixt, O., Head, S., Mondala, T., Scanlan, C., Huflejt, M.E., Alvarez, R., Bryan, M.C., Fazio, F., Calarese, D., Stevens, J., et al. (2004). Printed covalent glycan array for ligand profiling of diverse glycan binding proteins. Proc. Natl. Acad. Sci. U S A 101, 17033–17038.

Bovin, N.V. (1997). Carbohydrate-carbohydrate interaction. In Glycosciences: Status and Perspectives, H.-J. Gabius and S. Gabius, eds. (Weinheim: Chapman & Hall), pp. 277–289.

Bowman, K.G., and Bertozzi, C.R. (1999). Carbohydrate sulfotransferases: mediators of extracellular communication. Chem. Biol. 6, R9–R22.

Braccia, A., Villani, M., Immerdal, L., Niels-Christiansen, L.L., Nystrom, B.T., Hansen, G.H., and Danielsen, E.M. (2003). Microvillar membrane microdomains exist at physiological temperature. Role of galectin-4 as lipid raft stabilizer revealed by "superrafts". J. Biol. Chem. 278, 15679–15684.

Bum-Erdene, K., Leffler, H., Nilsson, U.J., and Blanchard, H. (2015). Structural characterization of human galectin-4 C-terminal domain: elucidating the molecular basis for recognition of glycosphingolipids, sulfated saccharides and blood group antigens. FEBS J. 282, 3348–3367.

Bum-Erdene, K., Leffler, H., Nilsson, U.J., and Blanchard, H. (2016). Structural characterisation of human galectin-4 N-terminal carbohydrate recognition domain in complex with glycerol, lactose, 3'-sulfo-lactose, and 2'-fucosyllactose. Sci. Rep. 6, 20289.

Bundle, D.R., Ling, C.C., and Zhang, P. (2003) Synthetic methods for the large scale production from glucose of analogs of sphingosine, azidosphingosine, ceramides, lactosyl ceramides and glycosyl phytosphingosine. International Patent Classification: C07C 247/08, International Application Number: PCT/CA03/00832, International Publication Number: WO 03/101937 A1, 11.12.2003.

Crich, D., Banerjee, A., Li, W., and Yao, Q. (2005). Improved synthesis of 1-benzenesulfinyl piperidine and analogs for the activation of thioglycosides in conjunction with trifluoromethanesulfonic anhydride. J. Carbohydr. Chem. 24, 415–424.

Danielsen, E.M., and van Deurs, B. (1997). Galectin-4 and small intestinal brush border enzymes form clusters. Mol. Biol. Cell 8, 2241–2251.

de Jong, C.G.H.M., Gabius, H.-J., and Baron, W. (2020). The emerging role of galectins in (re) myelination and its potential for developing new approaches to treat multiple sclerosis. Cell. Mol. Life Sci. 77, 1289–1317.

de Jong, C.G.H.M., Stancic, M., Pinxterhuis, T.H., van Horssen, J., van Dam, A.M., Gabius, H.-J., and Baron, W. (2018). Galectin-4, a negative regulator of oligodendrocyte differentiation, is persistently present in axons and microglia/macrophages in multiple sclerosis lesions. J. Neuropathol. Exp. Neurol. 77, 1024–1038.

Delacour, D., Gouyer, V., Zanetta, J.-P., Drobecq, H., Leteurtre, E., Grard, G., Moreau-Hannedouche, O., Maes, E., Pons, A., André, S., et al. (2005). Galectin-4 and sulfatides in apical membrane trafficking in enterocyte-like cells. J. Cell Biol. 169, 491–501.

Díez-Revuelta, N., Higuero, A.M., Velasco, S., Penas-de-la-Iglesia, M., Gabius, H.-J., and Abad-Rodríguez, J. (2017). Neurons define non-myelinated axon segments by the regulation of galectin-4-containing axon membrane domains. Sci. Rep. 7, 12246.

Eude-Le Parco, I., Gendronneau, G., Dang, T., Delacour, D., Thijssen, V.L., Edelmann, W., Peuchmaur, M., and Poirier, F. (2009). Genetic assessment of the importance of galectin-3 in cancer initiation, progression, and dissemination in mice. Glycobiology 19, 68–75.

Fukuda, M., Hiraoka, N., Akama, T.O., and Fukuda, M.N. (2001). Carbohydrate-modifying sulfotransferases: structure, function, and pathophysiology. J. Biol. Chem. 276, 47747–47750.

Gabius, H.-J., and Roth, J. (2017). An introduction to the sugar code. Histochem. Cell Biol. 147, 111–117.

García Caballero, G., Kaltner, H., Kutzner, T.J., Ludwig, A.-K., Manning, J.C., Schmidt, S., Sinowatz, F., and Gabius, H.-J. (2020). How galectins have become multifunctional proteins. Histol. Histopathol. 35, 509–539.

Göhler, A., André, S., Kaltner, H., Sauer, M., Gabius, H.-J., and Doose, S. (2010). Hydrodynamic properties of human adhesion/growth-regulatory galectins studied by fluorescence correlation spectroscopy. Biophys. J. 98, 3044–3053.

He, L., Wang, H., Garamus, V.M., Hanley, T., Lensch, M., Gabius, H.-J., Fee, C.J., and Middelberg, A. (2010). Analysis of monoPEGylated human galectin-2 by small-angle X-ray and neutron scattering: concentration dependence of PEG conformation in the conjugate. Biomacromolecules 11, 3504–3510.

Hemmerich, S., and Rosen, S.D. (2000). Carbohydrate sulfotransferases in lymphocyte homing. Glycobiology 10, 845–856.

Honke, K., Zhang, Y., Cheng, X., Kotani, N., and Taniguchi, N. (2004). Biological roles of sulfoglycolipids and pathophysiology of their deficiency. Glycoconj. J. 21, 59–62.

Hooper, L.V., Manzella, S.M., and Baenziger, J.U. (1997). The biology of sulfated oligosaccharides. In Glycosciences: Status and Perspectives, H.-J. Gabius and S. Gabius, eds. (Weinheim: Chapman & Hall), pp. 261–276.

Ideo, H., Matsuzaka, T., Nonaka, T., Seko, A., and Yamashita, K. (2011). Galectin-8-N-domain recognition mechanism for sialylated and sulfated glycans. J. Biol. Chem. 286, 11346–11355.

Ideo, H., Seko, A., Ishizuka, I., and Yamashita, K. (2003). The N-terminal carbohydrate recognition domain of galectin-8 recognizes specific glycosphingolipids with high affinity. Glycobiology 13, 713–723.

Ideo, H., Seko, A., and Yamashita, K. (2005). Galectin-4 binds to sulfated glycosphingolipids and carcinoembryonic antigen in patches on the cell surface of human colon adenocarcinoma cells. J. Biol. Chem. 280, 4730–4737.

Ideo, H., Seko, A., and Yamashita, K. (2007). Recognition mechanism of galectin-4 for cholesterol 3-sulfate. J. Biol. Chem. 282, 21081–21089.

Ishizuka, I. (1997). Chemistry and functional distribution of sulfoglycolipids. Prog. Lipid Res. 36, 245–319.

Kaltner, H., Abad-Rodríguez, J., Corfield, A.P., Kopitz, J., and Gabius, H.-J. (2019). The sugar code: letters and vocabulary, writers, editors and readers and biosignificance of functional glycan-lectin pairing. Biochem. J. 476, 2623–2655.

Kaltner, H., Toegel, S., García Caballero, G., Manning, J.C., Ledeen, R.W., and Gabius, H.-J. (2017). Galectins: their network and roles in immunity/tumor growth control. Histochem. Cell Biol. 147, 239–256.

Kamitori, S. (2018). Three-dimensional structures of galectins. Trends Glycosci. Glycotechnol. 30, SE41–SE50.

Krejciríková, V., Pachl, P., Fábry, M., Malý, P., Rezácová, P., and Brynda, J. (2011). Structure of the mouse galectin-4 N-terminal carbohydrate-recognition domain reveals the mechanism of oligosaccharide recognition. Acta Crystallogr. D67, 204–211.

Ledeen, R.W., Kopitz, J., Abad-Rodríguez, J., and Gabius, H.-J. (2018). Glycan chains of gangliosides: functional ligands for tissue lectins (siglecs/galectins). Progr. Mol. Biol. Transl. Sci. 156, 289–324.

Ludwig, A.-K., Michalak, M., Xiao, Q., Gilles, U., Medrano, F.J., Ma, H., FitzGerald, F.G., Hasley, W.D., Melendez-Davila, A., Liu, M., et al. (2019a). Design-functionality relationships for adhesion/growth-regulatory galectins. Proc. Natl. Acad. Sci. U S A 116, 2837–2842.

Ludwig, A.-K., Kaltner, H., Kopitz, J., and Gabius, H.-J. (2019b). Lectinology 4.0: altering modular (ga)lectin display for functional analysis and

biomedical applications. Biochim. Biophys. Acta *1863*, 935–940.

Michalak, M., Warnken, U., André, S., Schnölzer, M., Gabius, H.-J., and Kopitz, J. (2017). Detection of proteome changes in human colon cancer induced by cell surface binding of growth-inhibitory galectin-4 using quantitative SILAC-based proteomics. J. Proteome Res. *15*, 4412–4422.

Michalak, M., Warnken, U., Schnölzer, M., Gabius, H.-J., and Kopitz, J. (2019). Detection of malignancy-associated phosphoproteome changes in human colorectal cancer induced by cell surface binding of growth-inhibitory galectin-4. IUBMB Life *71*, 364–375.

Morelle, W., Stechly, L., André, S., van Seuningen, I., Porchet, N., Gabius, H.-J., Michalski, J.C., and Huet, G. (2009). Glycosylation pattern of brush border-associated glycoproteins in enterocyte-like cells: involvement of complex-type *N*-glycans in apical trafficking. Biol. Chem. *390*, 529–544.

Nabatov, A.A., Hatzis, P., Rouschop, K.M., van Diest, P., and Vooijs, M. (2013). Hypoxia inducible NOD2 interacts with 3-*O*-sulfogalactoceramide and regulates vesicular homeostasis. Biochim. Biophys. Acta *1830*, 5277–5286.

Percec, V., Leowanawat, P., Sun, H.J., Kulikov, O., Nusbaum, C.D., Tran, T.M., Bertin, A., Wilson, D.A., Peterca, M., Zhang, S., et al. (2013). Modular synthesis of amphiphilic Janus glycodendrimers and their self-assembly into glycodendrimersomes and other complex architectures with bioactivity to biomedically relevant lectins. J. Am. Chem. Soc. *135*, 9055–9077.

Phongsisay, V., Iizasa, E., Hara, H., and Yamasaki, S. (2015). 3-*O*-Sulfo-β-D-galactose moiety of endogenous sulfoglycolipids is a potential ligand for immunoglobulin-like receptor LMIR5. Mol. Immunol. *63*, 595–599.

Rao, U.S., and Rao, P.S. (2017). Surface-bound galectin-4 regulates gene transcription and secretion of chemokines in human colorectal cancer cell lines. Tumour Biol. *39*, 1010428317691687.

Rechreche, H., Mallo, G.V., Motalto, G., Dagorn, J.-C., and Iovanna, J.L. (1997). Cloning and expression of the mRNA of human galectin-4, an S-type lectin down-regulated in colorectal cancer. Eur. J. Biochem. *248*, 225–230.

Roberts, D.D., and Ginsburg, V. (1988). Sulfated glycolipids and cell adhesion. Arch. Biochem. Biophys. *267*, 405–415.

Róg, T., and Vattulainen, I. (2014). Cholesterol, sphingolipids, and glycolipids: what do we know about their role in raft-like membranes? Chem. Phys. Lipids *184*, 82–104.

Romero, A., and Gabius, H.-J. (2019). Galectin-3: is this member of a large family of multifunctional lectins (already) a therapeutic target? Expert Opin. Ther. Targets *23*, 819–828.

Satelli, A., Rao, P.S., Thirumala, S., and Rao, U.S. (2011). Galectin-4 functions as a tumor suppressor of human colorectal cancer. Int. J. Cancer *129*, 799–809.

Solís, D., Romero, A., Kaltner, H., Gabius, H.-J., and Díaz-Mauriño, T. (1996). Different architecture of the combining sites of two chicken galectins revealed by chemical-mapping studies with synthetic ligand derivatives. J. Biol. Chem. *271*, 12744–12748.

Sourkes, T.L. (2003). The Life and Work of J. L. W. Thudichum, 1829-1901: A Most Celebrated Exponent of the Art of Medicine and Chemistry (Osler Library, McGill University).

Stancic, M., Slijepcevic, D., Nomden, A., Vos, M.J., de Jonge, J.C., Sikkema, A.H., Gabius, H.-J., Hoekstra, D., and Baron, W. (2012). Galectin-4, a novel neuronal regulator of myelination. Glia *60*, 919–935.

Stechly, L., Morelle, W., Dessein, A.F., André, S., Grard, G., Trinel, D., Dejonghe, M.J., Leteurtre, E., Drobecq, H., Trugnan, G., et al. (2009). Galectin-4-regulated delivery of glycoproteins to the brush border membrane of enterocyte-like cells. Traffic *10*, 438–450.

Suzuki, Y., Toda, Y., Tamatani, T., Watanabe, T., Suzuki, T., Nakao, T., Murase, K., Kiso, M., Hasegawa, A., Tadano-Aritomi, K., et al. (1993). Sulfated glycolipids are ligands for a lymphocyte homing receptor, L-selectin (LECAM-1), binding epitope in sulfated sugar chain. Biochem. Biophys. Res. Commun. *190*, 426–434.

Takahashi, T., and Suzuki, T. (2012). Role of sulfatide in normal and pathological cells and tissues. J. Lipid Res. *53*, 1437–1450.

Thudichum, J.L.W. (1884). A Treatise on the Chemical Constitution of the Brain (Baillière, Tindall & Cox).

Tu, Z., Hsieh, H.W., Tsai, C.M., Hsu, C.W., Wang, S.G., Wu, K.J., Lin, K.I., and Lin, C.H. (2013). Synthesis and characterization of sulfated Gal-β1,3/4-GlcNAc disaccharides through consecutive protection/glycosylation steps. Chem. Asian J. *8*, 1536–1550.

Velasco, S., Díez-Revuelta, N., Hernández-Iglesias, T., Kaltner, H., André, S., Gabius, H.-J., and Abad-Rodríguez, J. (2013). Neuronal galectin-4 is required for axon growth and for the organization of axonal membrane L1 delivery and clustering. J. Neurochem. *125*, 49–62.

Vokhmyanina, O.A., Rapoport, E.M., André, S., Severov, V.V., Ryzhov, I., Pazynina, G.V., Korchagina, E., Gabius, H.-J., and Bovin, N.V. (2012). Comparative study of the glycan specificities of cell-bound human tandem-repeat-type galectins-4, -8 and -9. Glycobiology *22*, 1207–1217.

Vos, J.P., Lopes-Cardozo, M., and Gadella, B.M. (1994). Metabolic and functional aspects of sulfogalactolipids. Biochim. Biophys. Acta *1211*, 125–149.

Wasano, K., and Hirakawa, Y. (1999). Two domains of rat galectin-4 bind to distinct structures of the intercellular borders of colorectal epithelia. J. Histochem. Cytochem. *47*, 75–82.

Xiao, Q., Ludwig, A.-K., Romanò, C., Buzzacchera, I., Sherman, S.E., Vetro, M., Vértesy, S., Kaltner, H., Reed, E.H., Möller, M., et al. (2018). Exploring functional pairing between surface glycoconjugates and human galectins using programmable glycodendrimersomes. Proc. Natl. Acad. Sci. USA *115*, E2509–E2518.

Xiao, Q., Wang, Z., Williams, D., Leowanawat, P., Peterca, M., Sherman, S.E., Zhang, S., Hammer, D.A., Heiney, P.A., King, S.R., et al. (2016a). Why do membranes of some unhealthy cells adopt a cubic architecture? ACS Centr. Sci. *2*, 943–953.

Xiao, Q., Zhang, S., Wang, Z., Sherman, S.E., Moussodia, R.O., Peterca, M., Muncan, A., Williams, D.R., Hammer, D.A., Vértesy, S., et al. (2016b). Onion-like glycodendrimersomes from sequence-defined Janus glycodendrimers and influence of architecture on reactivity to a lectin. Proc. Natl. Acad. Sci. U S A *113*, 1162–1167.

Yamakawa, T., Kiso, N., Handa, S., Makita, A., and Yokoyama, S. (1962). On the structure of brain cerebroside sulfuric ester and ceramide dihexoside of erythrocytes. J. Biochem. *52*, 226–227.

Zhang, S., Moussodia, R.-O., Sun, H.J., Leowanawat, P., Muncan, A., Nusbaum, C.D., Chelling, K.M., Heiney, P.A., Klein, M.L., André, S., et al. (2014). Mimicking biological membranes with programmable glycan ligands self-assembled from amphiphilic Janus glycodendrimers. Angew. Chem. Int. Ed. *53*, 10899–10903.

Zhang, S., Moussodia, R.-O., Vértesy, S., André, S., Klein, M.L., Gabius, H.-J., and Percec, V. (2015). Unraveling functional significance of natural variations of a human galectin by glycodendrimersomes with programmable glycan surface. Proc. Natl. Acad. Sci. U S A *112*, 5585–5590.

Zhao, J., Liu, Y., Park, H.J., Boggs, J.M., and Basu, A. (2012). Carbohydrate-coated fluorescent silica nanoparticles as probes for the galactose/3-sulfogalactose carbohydrate-carbohydrate interaction using model systems and cellular binding studies. Bioconj. Chem. *23*, 1166–1173.

Supplemental Information

Probing sulfatide-tissue lectin recognition with functionalized glycodendrimersomes

Paul V. Murphy, Antonio Romero, Qi Xiao, Anna-Kristin Ludwig, Srinivas Jogula, Nadezhda V. Shilova, Tanuja Singh, Adele Gabba, Bilal Javed, Dapeng Zhang, Francisco J. Medrano, Herbert Kaltner, Jürgen Kopitz, Nicolai V. Bovin, Albert M. Wu, Michael L. Klein, Virgil Percec, and Hans-Joachim Gabius

Supplemental Figures and Legends
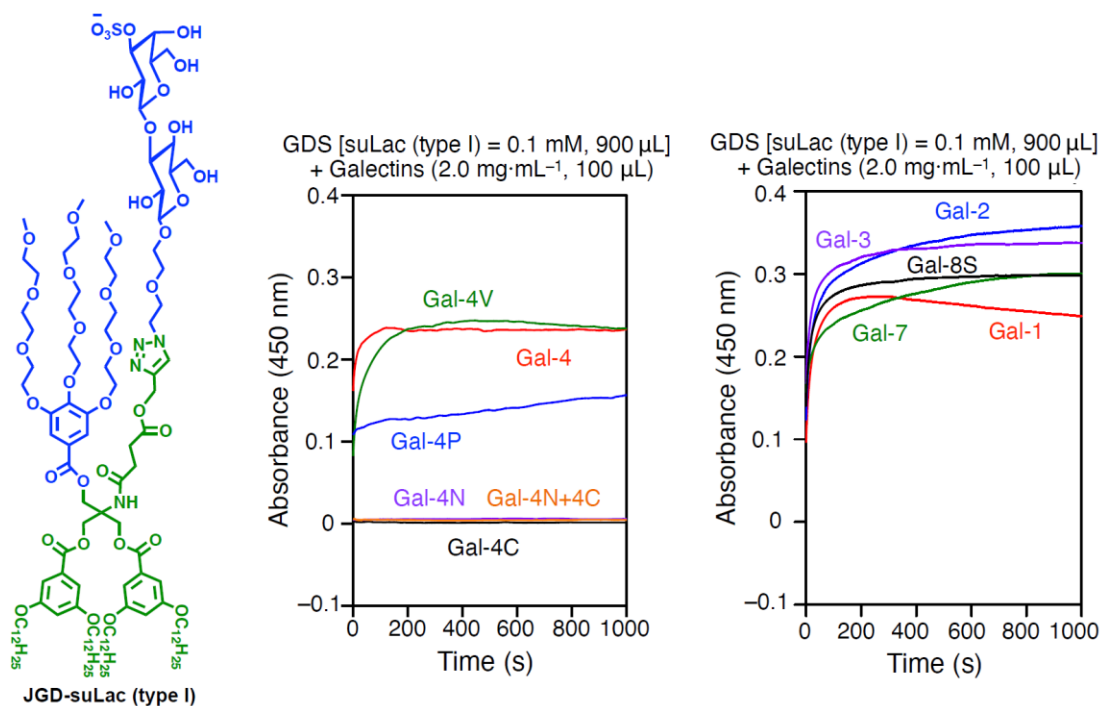
Figure S1. Course of aggregation of glycodendrimersomes (GDSs) presenting suLac (type I) with Gal-4 proteins and a panel of human galectins (2.0 mg/mL) in PBS (related to Scheme 1, Figure S3)
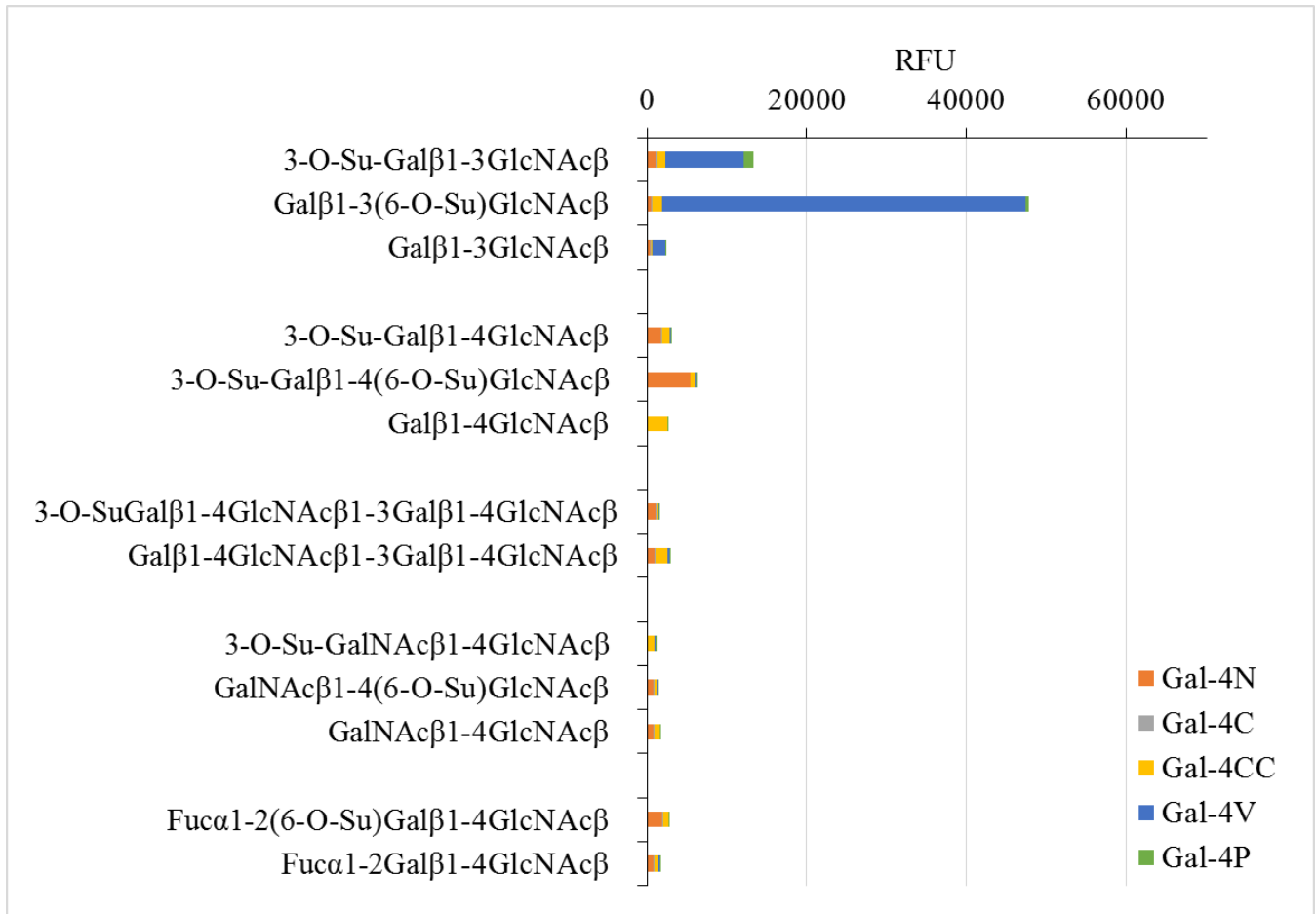
Figure S2. Stacked chart of signal intensities of binding of the two carbohydrate recognition domains (CRDs) of Gal-4, i.e. Gal-4N and Gal-4C, a Gal-4 variant constituted by two C CRDs and the variants with shortening of the 42 amino-acid-long linker to 16 amino acids (Gal-4V) and its removal (Gal-4P) to natural glycans (sulfated and parental structures) in an array (each colored part of the bar is the relative signal intensity (in relative units) for the given pair of protein and glycan). Related to Figure 1.

For details on data, see given link:

https://syncandshare.lrz.de/getlink/fiCpW4zo2HHDQfzEvRXvDu1L/Kopie_von_Gal-4_for_suppl_withoutTF.xlsx
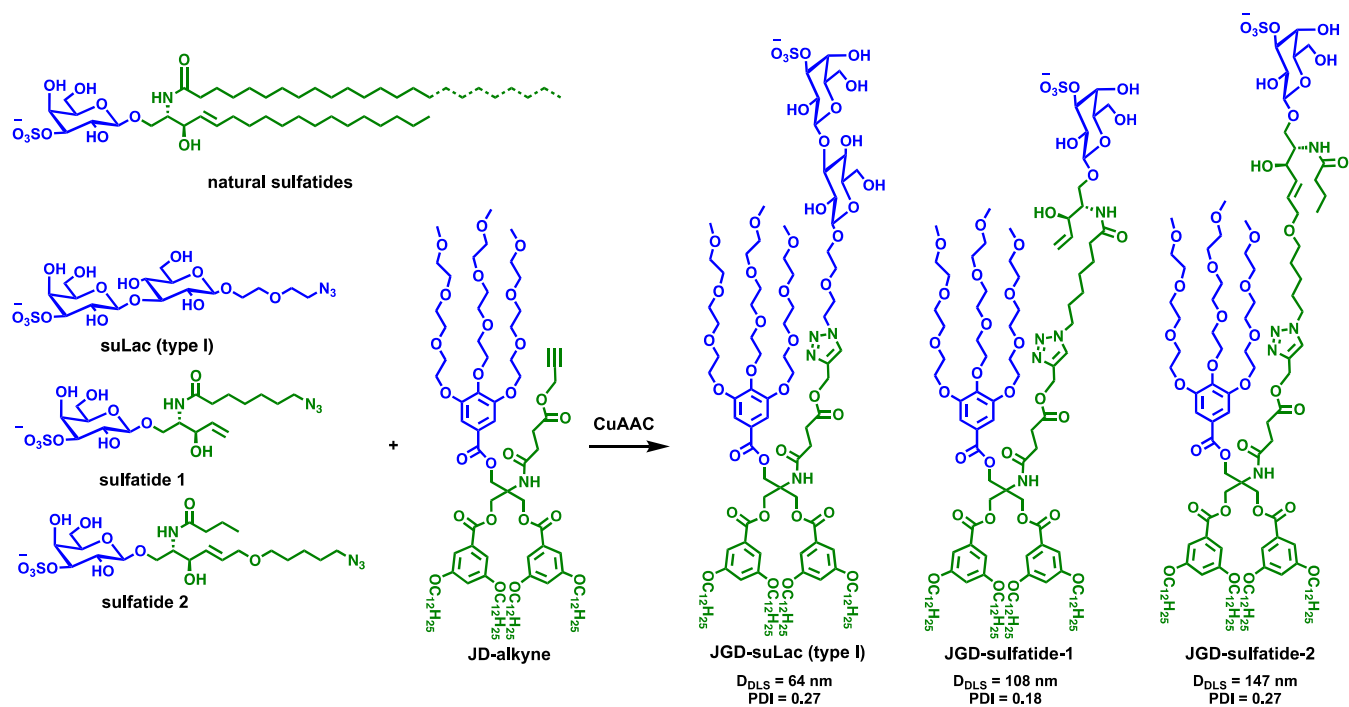
Figure S3. Synthesis of Janus glycodendrimers (JGDs) containing suLac (type I), sulfatide-1, and sulfatide-2 via copper-catalyzed azide-alkyne cycloaddition (CuAAC). Their diameter (D_{DLS}, in nm) and polydispersity (in the parentheses) were measured by dynamic light scattering (DLS) with 0.1 mM of sugar in PBS (pH = 7.4). (Related to Schemes 1-3, Figure 2, Figure S1)
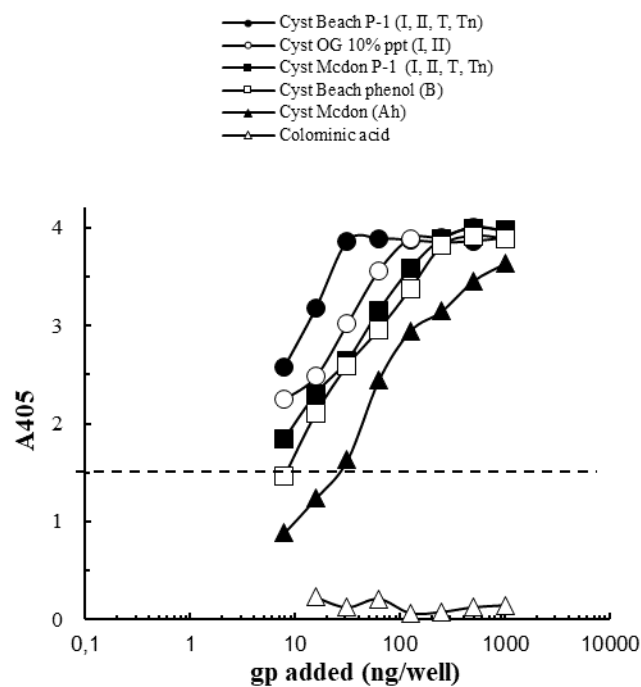
Figure S4. Binding of biotinylated Gal-4 (250 ng/well) to microtiter plates coated with six different glycoproteins. The standard deviation did not exceed 10%. Total volume of the assay was 50 μL. A_{405} was recorded after 24 h incubation. (Related to Figure 1)

Figure S5. Course of aggregation of co-assembled glycodendrimersomes (GDSs) with Gal-1 in PBS (pH = 7.4). Related to Figure 3.

Supplemental Tables

Table S1. Reactivity of hGal-4 for natural glycoproteins (gps)[a] (Related to Figure 1)

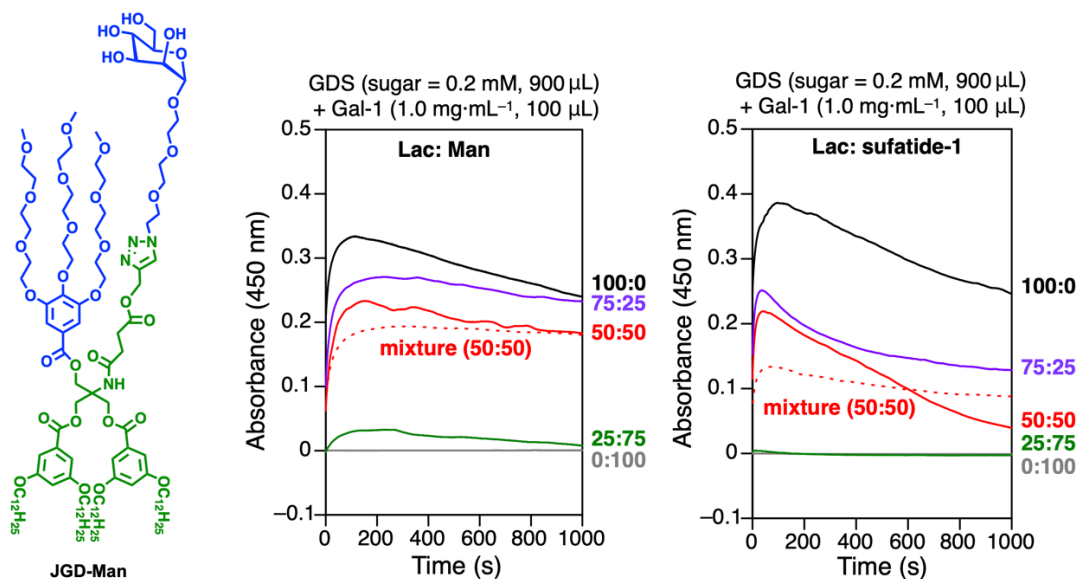| Glycoprotein (terminal epitope)[b]	1.5 (A_{405}) unit (ng)	Maximum A_{405} absorbance	
		Absorbance reading[c]	Binding intensity[c]
Histo-blood group precursor (equivalent) gps			
Cyst Beach P-1 (**I, II, T, Tn**)	0.3	3.7	5+
Cyst OG 10% ppt (**I, II**)	1.0	3.8	5+
Cyst Mcdon P-1 (**I, II, T, Tn**)	4.0	3.7	5+
Cyst JS 1st Smith degraded (**I/II**)	4.0	3.3	5+
Hog gastric mucin #21 (**I/II**)	4.0	3.3	5+
Cyst Tighe P-1 (**I/II**)	12.0	2.9	5+
Histo-blood group ABH-active gps			
Cyst MSS 10% 2x (**A$_h$**)	0.7	4.0	5+
Hog gastric mucin #9 (**A$_h$**, **H** on core 2 and I-active O-glycans)	1.2	4.1	5+
Hog gastric mucin #4 (**A$_h$**, **H** on core 2 and I-active O-glycans)	2.0	3.9	5+
Cyst MSM 10% ppt (**A$_h$**)	4.0	3.8	5+
Cyst 19 (**B$_h$**)	7.0	3.6	5+
Cyst Beach phenol insoluble (**B$_h$**)	8.0	3.7	5+
Cyst JS phenol insoluble (**H**)	22.0	3.2	5+
Cyst Mcdon (**A$_h$**)	30.0	3.4	5+
Lewis^a- and Lewis^b- active gps			
Cyst N-1 Le^a 20% 2x (**Le^a, Le^x**)	15.0	3.1	5+
Asialo HOC 350 (**Le^a**)	32.0	2.8	5+
Cyst Tighe phenol insoluble (**H, Le^a, Le^b, Le^x, Le^y**)	40.0	3.4	5+
HOC 350 (sialyl **Le^a**)	-	1.1	2+
Multi-antennary Galβ1-4GlcNAc (II) gps			
Bird nest asialo gp (**II, E, T, F**)	6.0	4.1	5+
Human asialo α$_1$-acid gp (m**II**)	28.0	2.5	5+
Asialofetuin (m**II/I, T$_α$**)	28.0	2.3	4+
Asialo THGP Sd (a$^+$) W. M. (**S, iII**)	30.0	3.4	5+
Bovine asialo α$_1$-acid gp (m**II**)	30.0	2.9	5+
Porcine thyroglobulin (α2-3/6 sialyl **mII**)	40.0	2.3	4+
Bird nest gp (sialyl **II, E, T$_α$, F$_α$**)	50.0	2.0	4+
THGP Sd (a$^+$) W. M. (**S, iII**)	60.0	2.7	5+
Porcine asialothyroglobulin (m**II**)	60.0	2.3	4+
Pneumococcus type 14 polysaccharide (i**II/Lac**)	100.0	2.0	4+
Asialo RSL (m**II**)	100.0	2.3	4+
Bovine asialolactoferrin (m**II, B**, LacdiNAc)	150.0	3.0	5+
Fetuin (α2-3/6 sialyl m**II/I**, sialyl/disialyl **T$_α$**)	-	0.7	+
Human α$_1$-acid gp (α2-3/6 sialyl m**II**)	-	0.4	±
Human asialolactoferrin (m**II**, i**II, Le^x**)	-	0.2	±
RSL (sialyl m**II**)	-	0.2	±
Bovine lactoferrin (α2-6 sialyl m**II, B**, LacdiNAc)	-	0.0	-
Bovine α$_1$-acid gp (sialyl m**II**)	-	0.0	-
T, Tn-containing gps			
Asialo PSM (**Tn, T$_α$, A$_h$, H**)	1.9	4.0	5+
PSM (sialyl **Tn, T$_α$ A$_h$, H**)	1.9	3.9	5+
Active antifreeze gp (**T$_α$**)	25.0	2.3	4+
Human asialoglycophorin (**T$_α$, Tn**, m**IIb/f**)	30.0	3.3	5+
Asialo BSM (**Tn**, GlcNAcβ1-3**Tn, T$_α$**)	50.0	2.5	5+
Asialo OSM (**Tn, T$_α$**, core 2 **II**)	80.0	2.4	4+
Human asialoagalactoglycophorin (**T$_α$, Tn**)	600.0	1.7	3+
Human glycophorin (sialyl **T$_α$, Tn**, α2-6 sialyl m**IIb/f**)	-	1.2	2+
BSM (sialyl **Tn**, GlcNAcβ1-3**Tn, T$_α$**)	-	1.0	2+

OSM (sialyl **Tn**, **T$_\alpha$**, core 2 **II**)	-	0.1	-

Table S2. Inhibitory potency of various glycoproteins on binding of hGal-4 (125 ng/50 μl) to a **I/II**-containing gp (Cyst beach P-1, 5 ng/50 μl)[a] (Related to Figure 1)

Inhibitor[b]	Quantity giving 50% inhibition (ng)[c]	Mass relative potency [d]
Histo-blood group precursor (equivalent) gps		
Cyst Beach P-1 (**I**, **II**, **T**, **Tn**)	0.3	7.0×10^5
Cyst OG 10% ppt (**I, II**)	0.9	2.3×10^5
Cyst Mcdon P-1 (**I, II, T, Tn**)	7.0	3.0×10^4
Cyst MSS 1st Smith (**I, II, Tn, T**)	7.0	3.0×10^4
Hog gastric mucin #14 (**I/II**)	20.0	1.0×10^4
Cyst JS 1st Smith degraded (**I/II**)	40.0	5.2×10^3
Hog gastric mucin #21 (**I/II**)	150.0	1.4×10^3
Cyst Tighe P-1 (**I/II**)	200.0	1.0×10^3
Histo-blood group ABH-active gps		
Hog gastric mucin #9 (**A$_h$**, **H**)	1.8	1.2×10^5
Hog gastric mucin #4 (**A$_h$**, **H**)	2.0	1.0×10^5
Cyst MSS 10% 2x (**A$_h$**)	2.0	1.0×10^5
Cyst Beach phenol insoluble (**B$_h$**)	30.0	7.0×10^3
Cyst 19 (**B$_h$**)	30.0	7.0×10^3
Cyst Mcdon (**A$_h$**)	110.0	1.9×10^3
Saccharides		
Tri-antennary Galβ1$\rightarrow$4GlcNAc (Tri-**II**)	1.0×10^4	21.0
Galβ1$\rightarrow$4Glc (**L**)	2.7×10^4	7.7
Galβ1$\rightarrow$4GlcNAc (**II**)	2.1×10^5	1.0
Gal	4.0×10^5	0.5
Multi-antennary Galβ1-4GlcNAc(II) gps		
Asialo bovine α1-acid GP (m**II**)	2.0×10^2	1.0×10^3
Asialo human α1-acid (m**II**)	2.0×10^2	1.0×10^3
Asialo fetuin (**II,T**)	2.5×10^3	8.0×10^1
Pneumococcus type 14 ps (i**II**)	>555.6 (36.6%)	–
Human α1-acid (α2-3/6 sialyl m**II**)	>277.8 (4%)	–
Bovine α1-acid (sialy m**II**)	>277.8 (2%)	–
Fetuin (sialy **II,T**)	>277.8 (8%)	–
T,Tn-containing gps		
Asialo BN in H$_2$O (**II, E, T, F**)	3.0	7.0×10^4
Asialo PSM (**T, Tn, A$_h$, H**)	20.0	1.0×10^4
Native BN (sialyl **II, E, T$_\alpha$, F$_\alpha$**)	>555.6 (33.4%)	–
PSM (sialy **T, Tn**)	>1388.9 (36.7%)	–

Table S3. Data collection and refinement statistics (Related to Figure 4)

Data collection	
Space group	C2
Wavelength (Å)	0.979257
Cell dimensions	
a, b, c (Å)	111.2, 40.2, 40.9
α, β, γ (°)	90, 99.9, 90
Resolution(Å)[a]	50.00 - 1.34 (1.42 - 1.34)
R_{merge}	3.3 (97.4)
CC 1/2	100 (82.3)
Completeness (%)	99.6 (98.3)
$<I/\sigma(I)>$	21.2 (1.5)
Redundancy	6.4 (6.2)
Mol/asymmetric unit	1
Refinement	
Resolution (Å)	50.0 - 1.34
No. reflections	39229
R_{work} / R_{free}	17.1 / 21.3
No. atoms (non-hydrogens)	
Protein	1254
Water	121
Sulfatide	23
PEG	10
Acetate ions	24
Average B factors (Å^2)	
Protein atoms	31.76
Water	42.26
Sulfatide	34.19
PEG	52.14
Acetate ions	54.80
R.m.s. deviations	
Bond lengths (Å)	0.009
Bond angles (°)	1.047
Ramachandran statistics	
Preferred (%)	98.05
Allowed (%)	1.95
Outliers (%)	0.00

[a]Values in parentheses are for highest-resolution shell.

Coordinates and structure factors have been deposited in the Protein Data Bank with accession code 6Z6Y.

Transparent Methods

Synthesis of clickable suLac(type 1), sulfatide-1 and sulfatide-2, the building blocks for JGD synthesis

Synthesis: Glycosylation between the known trichloroacetimidate **6** (Doyle et al., 2019) and diacetone-D-glucose (commercially available) gave the known β-glycosidic product **1** (60% yield) (Crich et al., 2005). After the hydrolysis of the acetonide groups and spontaneous rearrangement to the pyranoside form, the disaccharide was acetylated and then treated with 33% HBr in AcOH to give glycosyl bromide **2**. Reaction of **2** with diethylene glycol in the presence of silver carbonate in dichloromethane gave alcohol **3**. Reaction of this alcohol under Mitsunobu conditions gave the respective azide. Removal of the acyl protecting groups followed by regioselective sulfation in three steps gave **clickable suLac (type 1)**.
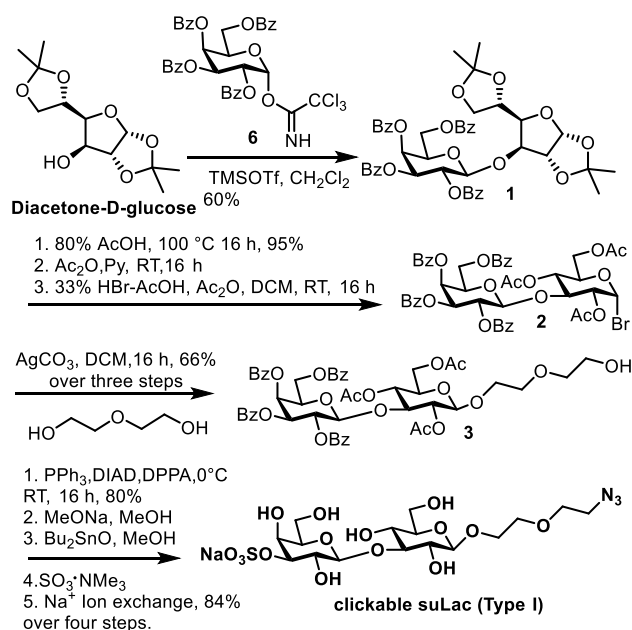
Scheme S1. Synthesis of clickable SuLac (Type-1)

The synthesis of the **clickable sulfatide 1** commenced from diol **4**, which was obtained as previously described from diacetone-D-glucose (Bundle et al.). The diol **4** was converted to the regioselectively benzoylated alcohol **5** via protection of its primary alcohol with a TBS group, then benzoylation and subsequent desilylation. Glycosidation with **6** (Doyle et al., 2019) provided **7**. Next reduction of the

azide using hydrogen sulfide (safety hazard[1]), followed by coupling with known 7-azido heptanoic acid (Wang et al., 2019) gave amide **8**. The removal of all benzoyl groups from **8** followed by regioselective sulfation gave **clickable sulfatide 1**. Yields for all steps are reported in the experimental details.
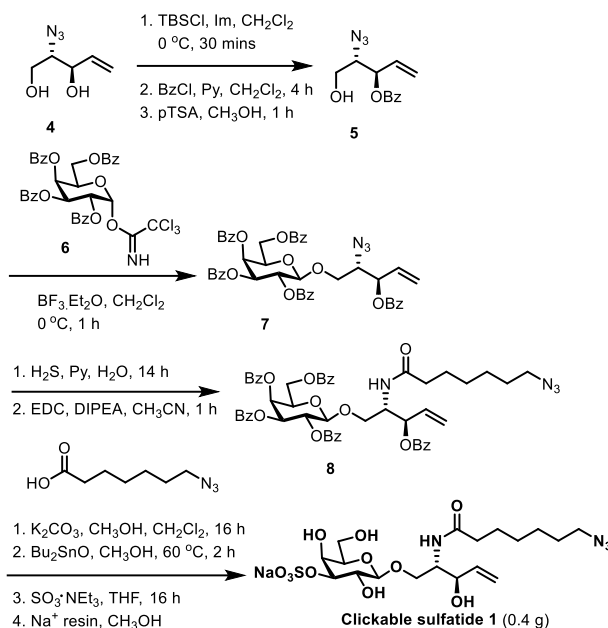
Scheme S2. Synthesis of Clickable Sulfatide-1

Preparation of **clickable sulfatide 2** was carried out from **11**, which was first prepared from D-galactal as described.[S6] The compatibility of protecting groups with certain reactions in the sequence, such as the alkylation and the requirement for orthogonal removal of PMB groups, complicated the sequence. Nevertheless, the clickable **sulfatide 2** could be prepared in ~0.4 g quantity. Thus the reduction of **11** followed by protection of the primary alcohol with a TBDPS group and subsequent Mitsunobu type substitution using azide, followed by TBDPS removal gave alcohol **12**. Alkylation was possible with TBS protected **13**, and gave **14**. We tried various methods for removal of the PMB groups, including use of DDQ, investigating a variety of conditions, but these were not successful. Use of TFA for this purpose also led to removal of TBS and so the latter was therefore exchanged for benzoate. Then successful removal of the two PMB groups was followed by reintroduction of the TBS group at the primary alcohol near the azide and the benzoate was exchanged for TBDPS. Benzoylation of the secondary alcohol followed by removal of the TBS group using aqueous HCl in THF gave acceptor **15**, which was glycosidated with **2** to give **16**. Subsequent reduction of the azide and coupling with butyric

---

[1]*Adequate precautions must be taken when using hydrogen sulfide as exposure to it at sufficiently high concentrations can seriously damage health or be fatal.*

acid gave **17**. Then removal of the TBDPS group followed by mesylation and substitution with azide gave **18**. Similar removal of all benzoates and sulfation as for other galactosides gave **clickable sulfatide-2**.
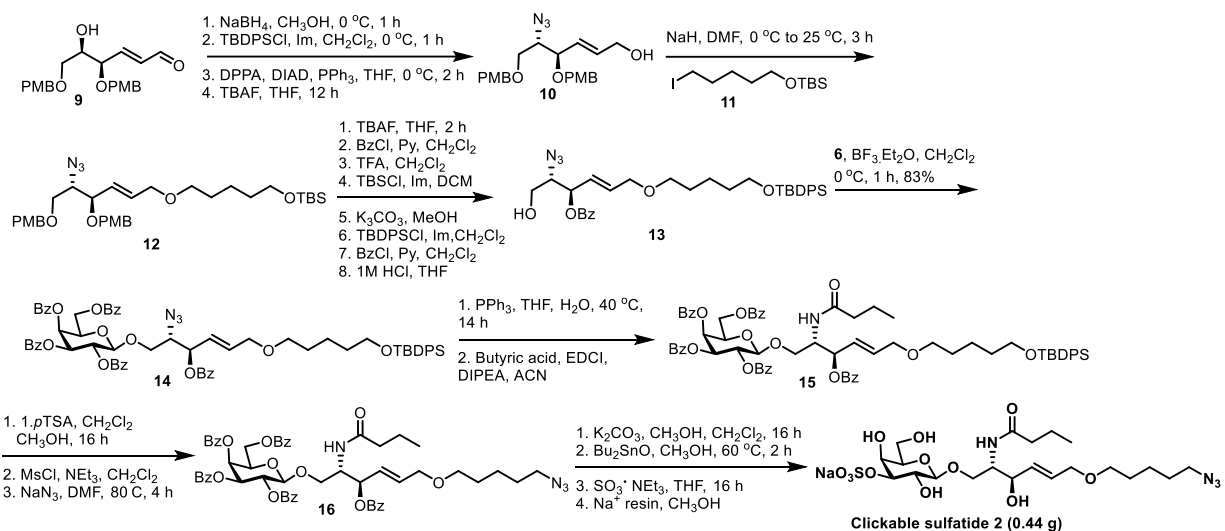
Scheme S3. Synthesis of Clickable Sulfatide-2

NMR spectra were recorded with 500 MHz Varian spectrometers. Chemical shifts are reported relative to internal Me_4Si in $CDCl_3$ (δ 0.0), HOD for D_2O (δ 4.84) or CD_2HOD (δ 3.31) for ^1H and $CDCl_3$ (77.16) or CD_3OD (49.05) for ^{13}C NMR spectra were processed and analysed using MestReNova software. ^1H-NMR signals were assigned with the aid of gCOSY. ^{13}C-NMR signals were assigned with the aid of APT, gHSQCAD and/or gHMBCAD. Coupling constants are reported in Hertz, with all J values reported uncorrected. Low- and high-resolution mass spectra were measured on a Waters LCT Premier XE Spectrometer, measuring in both positive and/or negative mode as, using MeCN, H_2O and/or MeOH as solvent. Thin layer chromatography (TLC) was performed on aluminium sheets precoated with silica gel 60 (HF254, E. Merck) and spots visualized by UV and charring with H_2SO_4-EtOH (1:20), cerium molybdate or phosphomolybdic acid staining agents. Flash chromatography was carried out with silica gel 60 (0.040-0.630 mm, E. Merck or Aldrich) and using a stepwise solvent polarity gradient (starting with the conditions indicated in each case and increasing the polarity as required), correlated with TLC mobility. Chromatography solvents, cyclohexane, EtOAc, CH_2Cl_2 and MeOH were used as obtained from suppliers (Fisher Scientific and Sigma-Aldrich). Anhydrous pyridine and DMF were purchased from Sigma Aldrich with other dried solvents (methanol, THF, dicholoromethane, toluene, diethyl ether) being used as obtained after treating with Pure Solv™ Solvent Purification System.

Detailed Synthetic Protocols

Preparation of 3   The glycoside **1** (382 mg) was dissolved in 6 mL of 80% AcOH in water and heated at 100 ºC for 16 h to yield intermediate pyranose (95%); ESI-HRMS: Calcd for $C_{40}H_{38}NaO_{15}$ $[M+Na]^+$ 781.2108; Found, 781.2147; ^1H NMR (500 MHz, CDCl$_3$): δ 8.07 (overlapped signals, 2H), 8.01 (overlapped signals, 3H), 7.79 (overlapped signals, 2H), 7.64 (t, J = 7.3 Hz, 1H), 7.58 – 7.49 (overlapped signals, 4H), 7.42 (overlapped signals, 5H), 7.29 – 7.22 (overlapped signals, 3H), 6.01 (s, 1H), 5.79 (t, J = 9.1 Hz, 1H), 5.62 (d, J = 12.8 Hz, 1H), 5.53 (s, 1H), 4.99 (d, J = 7.9 Hz, 1H), 4.57 (d, J = 5.9 Hz, 2H), 4.44 – 4.35 (overlapped signals, 2H), 4.23 (s, 1H), 4.20 – 4.15 (m, 1H), 4.15 – 4.09 (m, 1H), 3.88 (d, J = 11.7 Hz, 1H), 3.70 (dd, J = 11.5, 5.8 Hz, 1H); ^{13}C NMR (125 MHz, CDCl$_3$) δ 165.5, 165.4, 164.8, 163.2, 133.8, 133.7, 133.4, 133.4, 130.0, 129.9, 129.8, 129.6, 129.1, 128.9, 128.8, 128.7, 128.6, 128.5, 128.5, 128.3, 112.2, 105.2, 101.9, 83.6, 83.2, 79.9, 72.3, 71.3, 69.5, 68.8, 68.0, 64.3, 62.2. To this intermediate (1.25 g, 1.49 mmol) in pyridine (7 mL), Ac$_2$O (7 mL) was slowly added at 0 °C. The reaction mixture was stirred for 16 h at room temperature. The solvents were then removed by co-evaporation with toluene and the residue dissolved in dry dichloromethane (5.5 mL). The mixture was cooled to 0 °C, then 33% HBr in AcOH (1.85 mL) and Ac$_2$O (5mL) were added and the mixture left for 2 h at room temperature. The mixture was diluted with 10 mL dichloromethane and cold sat aq NaHCO$_3$ was added. The aqueous phase was extracted with dichloromethane (20 mL x 3). The combined organic phases were dried over Na$_2$SO$_4$ and the solvent removed under reduced pressure to give the residue which was the glycosyl bromide intermediate **2**.   The bromide obtained was dissolved in dry dichloromethane (13 mL), then diethyleneglycol (DEG, 2.6 mL, 27.5 mmol) and silver carbonate (640 mg, 2.33 mmol) were added. The mixture was stirred at 30 °C for 16 h in the dark. The mixture was passed through celite®, washing with water and dichloromethane. The phases were separated and the organic portion dried over Na$_2$SO$_4$ and the solvent removed under reduced pressure. Column chromatography (1:1 cyclohexane-EtOAc) gave **3** (955 mg, 66%); ESI-HRMS: Calcd for $C_{50}H_{52}O_{20}Na$, $[M+Na]^+$, 995.2950; Found, 995.2957; ^1H NMR (500 MHz, CDCl$_3$): δ 8.06 (overlapped signals, 4H), 7.85 (overlapped signals, 2H), 7.74 (overlapped signals, 2H), 7.63 (t, J = 7.5 Hz, 1H), 7.58 (t, J = 7.4 Hz, 1H), 7.52 (overlapped signals, 2H), 7.46 (overlapped signals, 3H), 7.41 (t, J = 7.4 Hz, 1H), 7.35 (overlapped signals, 2H), 7.21 (overlapped signals, 2H), 5.95 (d, J = 3.0 Hz, 1H), 5.67 – 5.57 (overlapped signals, 2H), 5.10 (t, J = 9.5 Hz, 1H), 4.95 (overlapped signals, 2H), 4.67 (dd, J = 10.8, 6.2

Hz, 1H), 4.42 (d, J = 7.8 Hz, 1H), 4.35 (dd, J = 10.8, 7.0 Hz, 1H), 4.30 (t, J = 6.6 Hz, 1H), 4.21 (dd, J = 12.2, 4.7 Hz, 1H), 4.15 (dd, J = 12.4, 2.7 Hz, 1H), 4.14 – 4.09 (m, 1H), 3.99 (t, J = 9.2 Hz, 1H), 3.66 (overlapped signals, 2H), 3.61 (dd, J = 11.0, 5.0 Hz, 1H), 3.58 – 3.54 (overlapped signals, 3H), 3.51 (overlapped signals, 2H), 2.09 (s, 3H), 2.07 (s, 3H), 1.93 (s, 3H); ^{13}C NMR (125 MHz, CDCl$_3$)δ 170.8, 169.1, 168.6, 166.0, 165.6, 165.4, 165.1, 133.7, 133.4, 133.3, 133.1, 129.9, 129.8, 129.7, 129.6, 129.4, 129.3, 128.9, 128.8, 128.5, 128.5, 128.3, 128.2, 101.1, 100.7, 78.3, 77.3, 77.0, 76.8, 72.5, 72.3, 71.7, 71.0, 70.1, 69.9, 68.3, 68.3, 67.8, 62.2, 61.6, 61.6, 20.9, 20.8, 20.7.

Preparation of clickable suLac (type 1)   To **3** (888 mg, 0.91 mmol) in THF (10 mL) at 0 ºC, PPh$_3$ (765 mg, 2.9 mmol) and DIAD (590 mg, 2.9 mmol) were added. The reaction mixture was stirred at 0 ºC until the solution became clear. DPPA (826 mg, 3.0 mmol, 3.3 eq.) was then added and the reaction was allowed to attain room temperature and stirred for 2 h. The mixture was diluted with EtOAc (100 mL) and washed with H$_2$O (3 x 15 mL). The organic portion was dried over Na$_2$SO$_4$ and the solvent removed under reduced pressure. Column chromatography (7:3 to 1:1 cyclohexane-EtOAc, gradient elution) gave the intermediate azide (725 mg, 80%); ESI-HRMS: Calcd for C$_{52}$H$_{50}$N$_3$O$_{19,}$ [M+H]$^+$, 1020.3039; Found, 1020.3043; ^{1}H NMR (500 MHz, CDCl$_3$) δ 8.10–8.03 (overlapped signals, 4H), 7.88–7.83 (overlapped signals, 2H), 7.74 (overlapped signals, 2H), 7.64 (t, J = 7.0 Hz, 1H), 7.59 (t, J = 7.5 Hz, 1H), 7.52 (overlapped signals, 2H), 7.46 (overlapped signals, 3H), 7.41 (t, J = 7.4 Hz, 1H), 7.35 (t, J = 7.8 Hz, 2H), 7.22 (overlapped signals, 2H), 5.95 (dd, J = 3.2, 1.1 Hz, 1H), 5.68 – 5.61 (m, 1H), 5.61 – 5.56 (m, 1H), 5.10 (t, J = 9.5 Hz, 1H), 4.95 (overlapped signals, 2H), 4.66 (dd, J = 11.0, 6.4 Hz, 1H), 4.43 (dd, J = 7.9, 1.0 Hz, 1H), 4.38 – 4.34 (m, 1H), 4.34 – 4.26 (m, 1H), 4.21 (dd, J = 12.2, 4.7 Hz, 1H), 4.15 (dd, J = 12.3, 2.5 Hz, 1H), 3.98 (t, J = 9.3 Hz, 1H), 3.85 (dt, J = 11.1, 3.8 Hz, 1H), 3.69 – 3.61 (overlapped signals, 2H), 3.61 – 3.55 (overlapped signals, 3H), 2.09 (s, 3H), 2.07 (s, 3H), 1.92 (s, 3H); ^{13}C NMR (125 MHz, CDCl$_3$): δ 169.0, 168.4, 166.0, 165.4, 165.1, 156.3, 155.8, 133.7, 133.4, 133.3, 133.1, 129.9, 129.8, 129.7 (2 signals), 129.5, 129.3, 128.9, 128.8, 128.5, 128.5, 128.3, 128.1, 101.1, 100.8, 78.3, 72.4, 72.0, 71.0, 70.4, 70.2, 70.1, 68.5, 68.3, 67.8, 62.2, 61.6, 50.8, 20.9, 20.8, 20.7. To the azide (700 mg, 0.7 mmol) in dry dichloromethane (7 mL), freshly prepared sodium methoxide in dry methanol was added until the pH was 10 and the solution was stirred at room temperature for 4 h. The solution was neutralized with an ion exchange resin (Dowex 50 × 8, H$^+$ form), filtered and concentrated to give the fully deacylated intermediate in quantitative yield. This intermediate and Bu$_2$SnO (227 mg, 0.912 mmol) were stirred in dry MeOH (30 mL) while heating at reflux under argon for 2 h. The solvent

was removed under reduced pressure and the resulting complex was treated with $Me_3N·SO_3$ (166 mg, 1.19 mmol) in dry THF (30 mL) at room temperature for 12 h. The solvent was evaporated off under reduced pressure, then the residue was dissolved in 1:1 $CHCl_3$-MeOH, and passed through a cation exchange resin column (Dowex 50 × 8 Na^+ form), eluting with 1:1 $CHCl_3$-MeOH. The solvents were then removed under reduced pressure and flash chromatography (8:2 to 7:3, $CHCl_3$-MeOH) gave the **clickable suLac (type 1)** (312 mg, 84%); ESI-HRMS: Calcd for $C_{16}H_{28}N_3O_{15}S$, $[M-Na]^-$, 534.1241; Found, 534.1245; ^{1}H NMR (500 MHz, CD_3OD) δ 4.63 (d, J = 7.8 Hz, 1H, H-1), 4.38 (d, J = 7.9 Hz, 1H, H-1), 4.26 (dd, J = 9.7, 3.2 Hz, 1H, galactose H-3), 4.23 (d, J = 2.6 Hz, 1H)., 4.01 (dt, J = 10.4, 4.4 Hz, 1H), 3.87 (d, J = 11.5 Hz, 1H), 3.82 – 3.74 (overlapped signals, 3H), 3.74 – 3.64 (overlapped signals, 6H), 3.65 – 3.55 (overlapped signals, 2H), 3.47 – 3.37 (overlapped signals, 4H), 3.35 – 3.32 (m, 1H); ^{13}C NMR (125 MHz, MeOD) δ 105.3, 103.7, 87.7, 81.3, 77.4, 76.6, 74.3, 71.2, 71.2, 70.8, 69.9, 69.6, 68.5, 62.5, 62.4, 51.7.

Preparation of 5   To stirred **4** (1 g, 6.9 mmol) in 25 mL dry dichloromethane at 0 °C under nitrogen, was added imidazole (0.71 g, 10.5 mmol) followed by TBSCl (1.16 g, 7.6 mmol). The mixture was stirred for 30 mins at 0 °C and then 10 mL H_2O was added and the mixture extracted with dichloromethane (2 x 10 mL). The organic portions were combined and dried over Na_2SO_4, and the solvent was removed at 30 °C, using a rotary evaporator (150 mm Hg).   The residue obtained was used in the next step, without further purification. A small portion was subjected to flash column chromatography with 15% EtOAc–cyclohexane as eluant to give sample for analysis; TLC: R_f 0.3 in 1:4 EtOAc-cyclohexane; HRMS: $[M+Cl]^-$ Calcd for $C_{11}H_{23}N_3O_2SiCl$ 292.1248, found 292.1252; ^{1}H NMR (500 MHz, $CDCl_3$): δ 5.97 – 5.84 (m, 1H), 5.39 (dp, J = 17.2, 1.4 Hz, 1H), 5.29 (dp, J = 10.6, 1.4 Hz, 1H), 4.29 (q, J = 5.6 Hz, 1H), 3.91 – 3.78 (overlapped signals, 2H), 3.43 (td, J = 5.7, 3.0 Hz, 1H), 2.50 (dd, J = 5.6, 1.7 Hz, 1H), 0.94 – 0.88 (overlapped signals, 9H), 0.10 (d, J = 1.8 Hz, 6H); ^{13}C NMR (125 MHz, $CDCl_3$): δ 136.5, 117.5, 73.3, 65.9, 63.5, 25.7, 18.1, -5.6. To the residue, taken up in 15 mL dry dichloromethane, at 0 °C under nitrogen, was added 3 mL pyridine followed by BzCl (1.2 mL, 10.5 mmol). The mixture was stirred for 4 h at room temperature and then sat aq $NaHCO_3$ solution was added at 0° C, and extracted with dichloromethane (2 x 15 mL). The combined organic portions dried over Na_2SO_4 and the solvent was removed under reduced pressure. The residue was used in the next step without further purification. A small portion was subjected to flash column chromatography (1:19 EtOAc–cyclohexane) to give a sample for analysis; TLC: R_f 0.2 in 1:19 EtOAc–cyclohexane; HRMS:

[2M+H]$^+$ Calcd for C$_{36}$H$_{55}$N$_6$O$_6$Si$_2$ 723.3722, found 723.3713; ^{1}H NMR (500 MHz, CDCl$_3$) δ 8.07 (overlapped signals, 2H), 7.59 (td, J = 7.4, 1.4 Hz, 1H), 7.46 (overlapped signals, 2H), 5.96 (dddd, J = 17.2, 10.5, 6.9, 1.3 Hz, 1H), 5.66 (ddt, J = 6.9, 4.6, 1.1 Hz, 1H), 5.46 (dq, J = 17.3, 1.1 Hz, 1H), 5.38 (dt, J = 10.5, 1.1 Hz, 1H), 3.89 – 3.67 (overlapped signals, 3H), 0.91 (overlapped signals, 10H), 0.08 (overlapped signals, J = 1.7 Hz, 6H).

^{13}C NMR (125 MHz, CDCl$_3$) δ 165.2, 133.3, 131.8, 129.7, 128.5, 120.2, 74.2, 65.5, 62.7, 25.7, 18.2, -5.5, -5.6. To this intermediate in 10 mL of MeOH, pTSA (0.13 g, 0.7 mmol) was added. After stirring for 1 h at room temperature, 5 mL sat aq NaHCO$_3$ solution was added and the mixture was extracted with dichloromethane (2 x 15 mL), the combined organic portions were dried over Na$_2$SO$_4$ and the solvent was removed under reduced pressure. Flash column chromatography, with 20% EtOAc–cyclohexane as eluant, gave **5** (1.2 g, 72% over 3 steps); TLC: R_f 0.2 in 1:4 EtOAc–cyclohexane; HRMS: [M+Cl]$^-$ Calcd for C$_{12}$H$_{13}$N$_3$O$_3$Cl 282.0645, found 282.0652; ^{1}H NMR (500 MHz, CDCl$_3$) δ 8.10 – 8.04 (overlapped signals, 2H), 7.63 – 7.56 (m, 1H), 7.47 (overlapped signals, 2H), 6.00 (ddd, J = 17.3, 10.5, 6.9 Hz, 1H), 5.68 (ddt, J = 7.1, 5.0, 1.1 Hz, 1H), 5.50 (dt, J = 17.2, 1.2 Hz, 1H), 5.41 (dt, J = 10.5, 1.1 Hz, 1H), 3.88 – 3.77 (overlapped signals, 2H), 3.69 (dd, J = 11.7, 7.1 Hz, 1H), 2.08 (s, 1H); ^{13}C NMR (125 MHz, CDCl$_3$) δ 165.4, 133.5, 131.8, 129.8, 129.5, 128.6, 120.5, 74.3, 65.8, 61.8.

Preparation of 7 To stirred **6** (4.0 g, 5.4 mmol), in 35 mL of dry dichloromethane at 0 ^{o}C under nitrogen, BF$_3$.Et$_2$O (0.7 mL, 5.4 mmol) was charged slowly. The mixture was stirred for 30 mins at 0 ^{o}C. Then compound **5** (0.9 g, 3.6 mmol) in 5 mL of dry dichloromethane was charged slowly and the mixture was stirred for 30 mins at 0 ^{o}C. Then 15 mL sat aq NaHCO$_3$ solution was added and the mixture was extracted with dichloromethane (2 x 30 mL), then the organic portions were combined and dried over Na$_2$SO$_4$, and the solvent was removed under reduced pressure. Flash column chromatography, using 14:86 EtOAc–cyclohexane as eluant, gave **7** (2.4 g, 81%) as a white solid; TLC: R_f 0.2 in 15:85 EtOAc–cyclohexane; HRMS [M+Na]$^+$ Calcd for C$_{46}$H$_{39}$N$_3$O$_{12}$Na 848.2431, found 848.2405; ^{1}H NMR (500 MHz, CDCl$_3$) δ 8.11 (overlapped signals, 2H), 8.06 – 7.94 (overlapped signals, 6H), 7.82 – 7.76 (overlapped signals, 2H), 7.66 – 7.60 (m, 1H), 7.58 – 7.53 (overlapped signals, 2H), 7.53 – 7.47 (overlapped signals, 3H), 7.43 (overlapped signals, 5H), 7.37 (overlapped signals, 2H), 7.27 – 7.24 (overlapped signals, 2H), 5.99 (dd, J = 3.4, 1.2 Hz, 1H), 5.92 – 5.80 (overlapped signals, 2H), 5.69 – 5.64 (m, 1H), 5.62 (dd, J = 10.4, 3.5 Hz, 1H), 5.32 (dt, J = 17.2, 1.2 Hz, 1H), 5.25 (dt, J = 10.6, 1.1 Hz, 1H), 4.90 (d, J = 7.9 Hz, 1H), 4.63 (dd, J = 11.1, 6.3 Hz, 1H), 4.38 (dd, J = 11.1, 6.6 Hz, 1H),

4.36 – 4.31 (m, 1H), 4.09 (dd, J = 10.2, 6.8 Hz, 1H), 4.01 (ddd, J = 6.7, 5.4, 4.2 Hz, 1H), 3.78 (dd, J = 10.2, 5.4 Hz, 1H); ^{13}C NMR (125 MHz, CDCl$_3$) δ 166.0, 165.6, 165.6, 165.1, 165.0, 163.6, 133.7, 133.3, 133.3, 133.3, 131.3, 130.1, 129.8, 129.8, 129.8, 129.7, 129.6, 129.3, 129.2, 128.9, 128.7, 128.7, 128.5, 128.5, 128.4, 128.4, 128.4, 128.3, 128.3, 120.5, 101.2, 74.5, 71.6, 71.5, 69.6, 8.0, 67.9, 63.1, 61.9.

Preparation of 8   H$_2$S gas (generated from Na$_2$S with dilute H$_2$SO$_4$) was bubbled, for 30 mins, to stirred **7** (2 g, 2.4 mmol) in 10 mL of pyridine and 10 mL of H$_2$O. The mixture was stirred for 14 h at room temperature and then bubbled with N$_2$ gas to remove the unreacted H$_2$S gas. It was then diluted with 20 mL of H$_2$O and extracted with dichloromethane (2 x 25 mL). The combined organic portions were dried over Na$_2$SO$_4$, then the solvent was removed under reduced pressure, to give the amine intermediate, which was used in the next step without further purification. This amine was dissolved in 15 mL of MeCN, and 1 mL of DIPEA was added as well as 7-azidoheptanoic acid (0.45 g, 2.6 mmol), followed by EDC (0.65 mL, 3.6 mmol). The mixture was stirred at room temperature for 1 h and then diluted with 10 mL sat aq NaHCO$_3$ and extracted with EtOAc (2x30 mL). The combined organic portions were dried over Na$_2$SO$_4$, and the solvent was removed under reduced pressure. Flash column chromatography with 1:3 EtOAc–cyclohexane, gave **8** (1.26 g, 56% over 2 steps) as a white solid; TLC: R_f 0.6 in 1:1 EtOAc–cyclohexane; HRMS [M+Na]$^+$ Calcd for C$_{53}$H$_{52}$N$_4$O$_{13}$Na 975.3429, found 974.3424; ^{1}H NMR (500 MHz, CDCl$_3$) δ 8.14 – 8.09 (overlapped signals, 2H), 8.08 – 8.02 (overlapped signals, 2H), 7.99 – 7.92 (overlapped signals, 4H), 7.77 (overlapped signals, 2H), 7.68 – 7.61 (m, 1H), 7.52 (overlapped signals, 5H), 7.47 – 7.33 (overlapped signals, 7H), 7.29 – 7.24 (overlapped signals, 2H), 5.92 (overlapped signals, 2H), 5.81 (d, J = 9.2 Hz, 1H), 5.74 (ddd, J = 10.3, 7.7, 2.1 Hz, 1H), 5.64 (overlapped signals, 2H), 5.43 – 5.36 (m, 1H), 5.26 (d, J = 10.7 Hz, 1H), 4.80 (dd, J = 7.7, 2.1 Hz, 1H), 4.53 (ddt, J = 9.7, 6.4, 3.2 Hz, 1H), 4.38 (ddd, J = 10.8, 5.9, 2.1 Hz, 1H), 4.31 – 4.17 (overlapped signals, 3H), 3.72 (dt, J = 10.0, 2.9 Hz, 1H), 3.20 (overlapped signals, 2H), 1.84 (overlapped signals, 2H), 1.55 – 1.39 (overlapped signals, 4H), 1.30 – 1.21 (overlapped signals, 2H), 1.15 (overlapped signals, 2H); ^{13}C NMR (125 MHz, CDCl$_3$) δ 172.5, 165.9, 165.5, 165.5, 165.1, 133.7, 133.6, 133.4, 133.3, 133.3, 133.1, 130.1, 130.0, 129.8, 129.7, 129.6, 129.3, 129.1, 129.0, 128.7, 128.6, 128.4, 128.3, 119.0, 100.9, 74.1, 71.3, 71.2, 70.2, 67.9, 67.1, 61.7, 51.3, 50.3, 36.2, 28.6, 28.5, 26.4, 25.2.

Preparation of clickable sulfatide-1   To stirred **8** (1.1 g, 1.1 mmol), in 10 mL of 1:1 MeOH–dichloromethane, was added K$_3$CO$_3$ (0.16 g, 1.1 mmol). The reaction mixture was stirred for 16 h at room temperature. The solvent was removed under reduced pressure and flash chromatography with

18:82 MeOH–dichloromethane, gave intermediate tetra-ol (0.4 g, 86%) as a white solid; TLC: R_f 0.2 in 15:85 MeOH–dichloromethane; HRMS [M+Na]$^+$ Calcd for $C_{18}H_{32}N_4O_8Na$ 455.2118, found 455.2124; ^{1}H NMR (500 MHz, CD$_3$OD) δ 7.89 (d, J = 9.1 Hz, 1H), 5.87 (dddd, J = 17.1, 10.5, 6.7, 1.0 Hz, 1H), 5.27 (dt, J = 17.2, 1.5 Hz, 1H), 5.14 (dq, J = 10.4, 1.3 Hz, 1H), 4.22 (dd, J = 7.5, 1.0 Hz, 1H), 4.19 – 4.12 (overlapped signals, 2H), 4.02 (dtt, J = 10.2, 5.0, 3.2 Hz, 1H), 3.82 (d, J = 3.3 Hz, 1H), 3.76 (dd, J = 11.3, 7.0 Hz, 1H), 3.71 (dd, J = 11.3, 5.1 Hz, 1H), 3.61 (dd, J = 10.3, 3.5 Hz, 1H), 3.56 – 3.49 (overlapped signals, 2H), 3.47 (dd, J = 9.8, 3.3 Hz, 1H), 3.27 (overlapped signals 2H), 2.20 (overlapped signals, 2H), 1.59 (overlapped signals, 4H), 1.37 (overlapped signals, 4H); ^{13}C NMR (125 MHz, CD$_3$OD) δ 174.7, 138.2, 115.5, 103.9, 75.4, 73.4, 71.8, 71.2, 68.9, 68.3, 61.1, 53.3, 51.0, 35.6, 28.4, 28.3, 26.1, 25.4; To this tetra-ol (0.3 g, 0.7 mmol) in 15 mL dry MeOH, was added Bu$_2$SnO (0.26 g, 1.0 mmol). The reaction mixture was heated at 60°C for 2 h. Then the solvent was removed under reduced pressure, and this was followed by drying under high vacuum for 30 mins. To well dried residue, which had been taken up in 15 mL dry THF, was added SO$_3$.NEt$_3$ (0.19 g, 1.4 mmol). The reaction mixture was stirred for 16 h at room temperature and then the solvent was removed under reduced pressure and the residue dissolved in 20 mL of 1:1 MeOH–dichloromethane and passed through a small bed of Na$^+$ resin, to form the sodium salt. The solvent was removed under reduced pressure and flash column chromatography with 20% MeOH–dichloromethane, gave **clickable sulfatide-1** (0.33 g, 91%); TLC: R_f 0.2 in 20% MeOH–dichloromethane; HRMS [M+H]$^+$ Calcd for $C_{18}H_{32}N_4O_{11}NaS$ 535.1686, found 535.1689; ^{1}H NMR (500 MHz, CD$_3$OD) δ 5.86 (dddd, J = 17.2, 10.4, 6.7, 1.8 Hz, 1H), 5.27 (dq, J = 17.3, 1.7 Hz, 1H), 5.13 (dq, J = 10.4, 1.6 Hz, 1H), 4.33 (dd, J = 7.8, 1.8 Hz, 1H), 4.27 – 4.14 (overlapped signals, 4H), 3.99 (dq, J = 8.2, 3.2, 2.6 Hz, 1H), 3.73 (overlapped signals, 3H), 3.63 – 3.54 (overlapped signals, 2H), 3.28 (overlapped signals, 2H), 2.20 (overlapped signals, 2H), 1.66 – 1.55 (overlapped signals, 4H), 1.45 – 1.30 (overlapped signals, 4H); ^{13}C NMR (125 MHz, CD$_3$OD) δ 174.63, 138.2, 115.5, 103.7, 80.4, 75.0, 71.7, 69.6, 68.3, 67.1, 61.0, 53.2, 51.0, 35.6, 28.4, 28.3, 26.1, 25.4.

Preparation of 10   To aldehyde **9** (14 g, 36 mmol) in 1:10 MeOH–THF (55 mL) at 0 ^{o}C was added, in a portionwise manner, NaBH$_4$ (1.51 g, 39.9 mmol). The mixture was stirred at room temperature for 1 h and then 30 mL of sat NH$_4$Cl solution was added at 0 ^{o}C, and the resulting mixture then extracted with EtOAc (2 x 150 mL). The organic layers were combined and washed with 60 mL of sat brine solution and the organic layer dried over Na$_2$SO$_4$. Flash column chromatography with 3:2 EtOAc–cyclohexane, gave intermediate allylic alcohol (11.4 g, 81%) as a colourless oil; TLC: R_f 0.1 in 1:1 EtOAc–cyclohexane; HRMS: [M+Na]$^+$ Calcd for $C_{22}H_{28}O_6Na$ 411.1784, found 411.1776; ^{1}H NMR (500 MHz,

CDCl$_3$): δ 7.22 (overlapped signals, 4H), 6.86 (overlapped signals, 4H), 5.87 (dt, J = 15.6, 5.2Hz, 1H), 5.64 (ddt, J = 15.7, 7.8, 1.6 Hz, 1H), 4.55 (d, J = 11.2 Hz, 1H), 4.47 (d, J = 11.6 Hz, 1H), 4.41 (d, J = 11.6 Hz, 1H), 4.28 (d, J = 11.3 Hz, 1H), 4.13 (overlapped signals, 2H), 3.92 (dd, J = 7.8, 6.1 Hz, 1H), 3.79 (overlapped signals, 6H), 3.73 (m, 1H), 3.52 (dd, J = 10.0, 4.1 Hz, 1H), 3.44 (dd, J = 10.0, 5.53 Hz, 1H), 2.78 (br s, 1H), 1.81 (br s, 1H); ^{13}C NMR (125 MHz, CDCl$_3$): δ 159.3, 159.3, 134.3, 130.1, 130.1, 129.5, 129.5, 127.8, 113.8, 113.8, 79.4, 73.0, 73.0, 70.3, 70.1, 62.7, 55.3. To this diol (10 g, 26 mmol) in 60 mL of dry CH$_2$Cl$_2$ at 0 °C under N$_2$ were added imidazole (2.6 g, 39 mmol) and TBDPSCl (7.4 mL, 28 mmol) at the same temperature. The reaction mixture was stirred at room temperature for 1 h, then diluted with 40 mL of water and extracted with CH$_2$Cl$_2$ (2 x 60 mL). The combined organic portions were dried over Na$_2$SO$_4$ and the solvent removed under reduced pressure. Flash column chromatography with 1:9 EtOAc–cyclohexane, gave the silylated intermediate (15.2 g, 94%) as a colourless liquid; TLC: R_f 0.2 in 1:4 EtOAc–cyclohexane; HRMS: [M+Na]$^+$ Calcd for C$_{38}$H$_{46}$O$_6$SiNa 649.2961, found 649.2938; ^{1}H NMR (500 MHz, CDCl$_3$): δ 7.71 – 7.65 (overlapped signals, 4H), 7.46 – 7.39 (overlapped signals, 2H), 7.37 (overlapped signals, 4H), 7.22 (overlapped signals, 4H), 6.85 (overlapped signals, 4H), 5.82 (dt, J = 15.5, 4.4 Hz, 1H), 5.69 (dd, J = 15.6, 7.9 Hz, 1H), 4.54 (d, J = 11.2 Hz, 1H), 4.47 (d, J = 11.7 Hz, 1H), 4.40 (d, J = 11.7 Hz, 1H), 4.29 – 4.20 (overlapped signals, 2H), 3.91 (t, J = 7.3 Hz, 1H), 3.80 (s, 3H), 3.77 (s, 3H), 3.74 – 3.68 (m, 1H), 3.53 (dd, J = 10.1, 3.5 Hz, 1H), 3.41 (dd, J = 10.1, 5.4 Hz, 1H), 2.68 (d, J = 3.5 Hz, 1H), 1.07 (s, 9H); ^{13}C NMR (125 MHz, CDCl$_3$): δ 159.2, 159.2, 135.5, 134.6, 133.6, 133.6, 130.2, 129.7, 129.6, 129.4, 127.7, 126.4, 113.8, 113.7, 79.7, 73.1, 70.2, 70.1, 63.7, 55.3, 55.2, 26.8, 19.3; To this intermediate (12 g, 19 mmol) in 100 mL of dry THF at 0 °C under nitrogen were added PPh$_3$ (10.0 g, 38.3 mmol) and DIAD (7.5 mL, 38.3 mmol) and the mixture was stirred for 30 mins at 0 °C, and then DPPA (8.3 mL, 38.3 mmol) was added. The reaction mixture was stirred for 1 hour. Then reaction mixture was diluted with 50 mL water and extracted with dichloromethane (2 x 80 mL), the organic portions were combined and washed with 40 mL of sat brine solution, dried over Na$_2$SO$_4$ and the solvent was removed under reduced pressure. Flash column chromatography with 1:19 EtOAc–cyclohexane, gave the intermediate azide (10.7 g, 86%) as a colourless liquid; TLC: R_f 0.6 in 1:4 EtOAc–cyclohexane; HRMS: [M+Na]$^+$ Calcd for C$_{38}$H$_{45}$N$_3$O$_5$SiNa 674.3026, found 674.3011; ^{1}H NMR (500 MHz, CDCl$_3$): δ 7.76 – 7.70 (overlapped signals, 3H), 7.48– 7.37 (overlapped signals, 9H), 7.32 – 7.20 (overlapped signals, 10H), 6.92 – 6.86 (overlapped signals, 3H), 5.86 (dt, J = 15.4, 3.9 Hz, 1H), 5.79 (dd, J = 15.4, 7.8 Hz, 1H), 5.25 (hept, J = 6.3 Hz, 1H), 4.55 (d, J = 11.5 Hz, 1H), 4.51–4.44 (overlapped signals, 2H), 4.29 (overlapped signals, 2H), 3.98 (dd, J = 7.7,

5.4 Hz, 1H), 3.80 (overlapped signals, 6H), 3.69 – 3.55 (overlapped signals, 3H), 1.11 (s, 9H); ^{13}C NMR (125 MHz, CDCl$_3$): δ 159.3, 159.2, 149.9, 149.8, 135.5, 135.5, 135.1, 133.6, 133.5, 130.1, 130.1, 129.9, 129.7, 129.3, 129.3, 127.7, 126.1, 126.1, 126.1, 120.2, 120.2, 113.8, 113.8, 78.5, 73.0, 70.0, 69.0, 64.3, 63.6, 55.2, 55.2, 26.9, 26.8, 21.6, 19.3. To this intermediate (8 g, 12 mmol) in 30 mL of THF under nitrogen, was added 1.0 M TBAF in THF (18.4 mL, 18.4 mmol). The reaction mixture was stirred at room temperature for 12 h. Then the reaction mixture was diluted with 30 mL of water and extracted with EtOAc (2 x 60 mL). The organic portions were then combined and washed with 40 mL of sat brine solution, dried over Na$_2$SO$_4$ and solvent was removed under reduced pressure. Flash column chromatography with 25% EtOAc–cyclohexane, gave **10** (4.61 g, 91%) as a colourless liquid; TLC: R_f 0.2 in 30:70 EtOAc–cyclohexane; HRMS: [M+Na]$^+$ Calcd for C$_{22}$H$_{27}$N$_3$O$_5$Na 436.1848, found 436.1836; ^{1}H NMR (500 MHz, CDCl$_3$): δ 7.22 (overlapped signals, 4H), 6.865 (overlapped signals, 4H), 5.90 (dt, J = 15.7, 5.1 Hz, 1H), 5.68 (dd, J = 15.6, 7.9 Hz, 1H), 4.53 (d, J = 11.4 Hz, 1H), 4.49 – 4.41 (overlapped signals, 2H), 4.293 (d, J = 11.4 Hz, 1H), 4.19 (d, J = 5.1 Hz, 2H), 3.96 (dd, J = 8.0, 5.6 Hz, 1H), 3.80 (overlapped signals, 6H), 3.59 (overlapped signals, 3H), 1.716 (s, 1H); ^{13}C NMR (125 MHz, CDCl$_3$): δ 159.3, 159.2, 135.1, 129.9, 129.8, 129.3, 129.3, 127.3, 113.8, 113.8, 78.4, 73.0, 70.2, 68.9, 64.2, 62.7, 55.3, 21.9.

Preparation of 12   To stirred **10** (5 g, 12 mmol) in 60 mL dry DMF at 0 ^{o}C under nitrogen, was added NaH (0.87 g, 36 mmol). The mixture was stirred for 1 h at 0 ^{o}C and then **11** (Furstner et al., 2007) (7.94 g, 24.2 mmol) in 20 mL of dry DMF was added over 10 min. The mixture was stirred for 2 h and then 30 mL of water was cautiously added at 0 ^{o}C, followed by extraction with EtOAc (2 x 60 mL). The combined organic portions were dried over Na$_2$SO$_4$, and the solvent was removed under reduced pressure. Flash column chromatography with 1:9 EtOAc–cyclohexane, gave **12** (5.32 g, 92% based on recovered **10**) as a colourless liquid and also recovered **10** (1.1 g); TLC: R_f 0.5 in 20% EtOAc–cyclohexane; HRMS: [M+Na]$^+$ Calcd for C$_{33}$H$_{51}$N$_3$O$_6$SiNa 636.3445, found 636.3441; ^{1}H NMR (500 MHz, CDCl3) δ 7.27 – 7.17 (overlapped signals, 4H), 6.861 (overlapped signals, 4H), 5.822 (dt, J = 15.7, 5.5 Hz, 1H), 5.66 (dd, J = 15.6, 8.1 Hz, 1H), 4.53 (d, J = 11.4 Hz, 1H), 4.45 (overlapped signals, 2H), 4.28 (d, J = 11.4 Hz, 1H), 4.01 (overlapped signals, 2H), 3.94 (dd, J = 8.0, 5.3 Hz, 1H), 3.80 (overlapped signals, 6H), 3.66 – 3.51 (overlapped signals, 6H), 3.43 (overlapped signals, 2H), 1.65–1.59 (overlapped signals, 2H), 1.54 (overlapped signals, 2H), 1.39 (overlapped signals, 2H), 0.89 (s, 9H), 0.044 (overlapped signals, 6H); ^{13}C NMR (125 MHz, CDCl$_3$) δ 159.3, 159.2, 133.0, 130.0, 129.9,

129.3, 129.3, 128.4, 113.8, 113.8, 78.5, 73.0, 70.5, 70.5, 70.1, 69.0, 64.2, 63.1, 55.2, 32.7, 29.5, 26.9, 26.0, 22.4, 18.3, -5.3.

Preparation of 13   To stirred **12** (5.0 g, 8.4 mmol) in 40 mL of THF under nitrogen, was added TBAF 1M in THF (12.2 mL, 12.2 mmol). The reaction mixture was stirred for 2 h at room temperature. Then the mixture was diluted with 20 mL of water and extracted with EtOAc (2 x 60 mL), the organic portions were combined and washed with 30 mL of sat brine solution and the organic layer dried over Na_2SO_4. The solvent was removed under reduced pressure and flash column chromatography, with 2:3 EtOAc–cyclohexane, gave intermediate alcohol (3.82 g, 94%) as a colourless liquid; TLC: R_f 0.4 in 1:1 EtOAc–cyclohexane; HRMS: $[M+Na]^+$ Calcd for $C_{27}H_{37}N_3O_6Na$ 522.2580, found 522.2576; ^1H NMR (500 MHz, CDCl$_3$) δ 7.22 (overlapped signals, 4H), 6.86 (overlapped signals, 4H), 5.82 (dt, J = 15.6, 5.4 Hz, 1H), 5.66 (dd, J = 15.6, 8.1 Hz, 1H), 4.53 (d, J = 11.5Hz, 1H), 4.50 (overlapped signals, 2H), 4.28 (d, J = 11.4 Hz, 1H), 4.01 (overlapped signals, 2H), 3.94 (dd, J = 8.0, 5.4 Hz, 1H), 3.80 (overlapped signals, 6H), 3.68 − 3.57 (overlapped signals, 4H), 3.54 (dd, J = 9.8, 6.9 Hz, 1H), 3.41 (overlapped signals, 2H), 1.67 − 1.58 (overlapped signals, 5H), 1.44 (overlapped signals, 2H); ^{13}C NMR (125 MHz, CDCl$_3$) δ 159.3, 159.2, 132.9, 129.9, 129.9, 129.3, 129.3, 128.5, 113.8, 113.8, 78.5, 73.0, 70.4, 70.3, 70.2, 69.0, 64.2, 62.8, 55.2, 32.5, 29.4, 22.4. To this alcohol intermediate (3.6 g, 7.2 mmol) in 40 mL dry dichloromethane under nitrogen at 0 °C, was added NEt$_3$ (3.01 mL, 21.61 mmol) followed by slow addition of BzCl (1.25 mL, 10.8 mmol). The reaction mixture was stirred for 1 h at room temperature, and then, cautiously, 5 mL of sat aq NaHCO$_3$ solution at 0 °C was added. The mixture was then diluted with 15 mL water and extracted with dichloromethane (2 x 50 mL). The combined organic portions were dried over Na_2SO_4 and the solvent was removed under reduced pressure. Flash column chromatography with 15% EtOAc–cyclohexane, gave a benzoylated intermediate (4.02 g, 93%) as a colourless syrup; TLC: R_f 0.3 in 20% EtOAc–cyclohexane; HRMS: $[M+Na]^+$ Calcd for $C_{34}H_{41}N_3O_7Na$ 626.2842, found 626.2833; ^1H NMR (500 MHz, CDCl$_3$) δ 8.04 (overlapped signals, 2H), 7.541 (t, J = 7.4 Hz, 1H), 7.425 (overlapped signals, 2H), 7.21 (overlapped signals, 4H), 6.90 − 6.82 (overlapped signals, 4H), 5.82 (dt, J = 15.6, 5.4 Hz, 1H), 5.66 (dd, J = 15.7, 8.0 Hz, 1H), 4.53 (d, J = 11.4 Hz, 1H), 4.44 (d, J = 2.6 Hz, 2H), 4.33 (overlapped signals, 2H), 4.28 (d, J = 11.4 Hz, 1H), 4.015 (overlapped signals, 2H), 3.94 (dd, J = 8.0, 5.3 Hz, 1H), 3.79 (overlapped signals, 6H), 3.64 − 3.56 (overlapped signals, 2H), 3.533 (dd, J = 9.6, 6.7 Hz, 1H), 3.46 (overlapped signals, 2H), 1.81 (overlapped signals, 2H), 1.68 (overlapped signals, 2H), 1.52 (overlapped signals, 2H); ^{13}C NMR (125 MHz, CDCl$_3$) δ

166.6, 159.3, 159.2, 132.9, 132.8, 130.4, 129.9, 129.9, 129.5, 129.3, 129.3, 128.5, 128.3, 113.8, 113.8, 78.4, 73.0, 70.5, 70.2, 70.2, 69.0, 64.9, 64.2, 55.2, 29.3, 28.6, 22.8.

To this benzoylated intermediate (3.8 g, 6.3 mmol) in dry 80 mL dichloromethane under nitrogen at 0 $^{\circ}$C, was added slowly 8 mL of trifluoroacetic acid. Stirring was continued at the same temperature for 2 h and then the volatile components were removed under reduced pressure at room temperature (avoiding heating). Flash column chromatography with 50% EtOAc–cyclohexane gave a diol (1.87 g, 82%) as a colourless syrup; TLC: R_f 0.1 in 50% EtOAc–cyclohexane; HRMS: [M+Na]$^+$ Calcd for $C_{18}H_{25}N_3O_5Na$ 386.1692, found 386.1677; ^{1}H NMR (500 MHz, CDCl$_3$) δ 8.03 (overlapped signals, 2H), 7.55 (t, J = 7.2 Hz, 1H), 7.43 (overlapped signals, 2H), 5.90 (dt, J = 15.6, 5.3 Hz, 1H), 5.79 (dd, J = 15.6, 6.5 Hz, 1H), 4.35 – 4.28 (overlapped signals, 3H), 3.99 (overlapped signals, 2H), 3.80 (overlapped signals, 2H), 3.49 (t, J = 5.2 Hz, 1H), 3.46 (overlapped signals, 2H), 2.53 (overlapped signals, 2H), 1.79 (overlapped signals, 2H), 1.66 (overlapped signals, 2H), 1.52 (overlapped signals, 2H); ^{13}C NMR (125 MHz, CDCl$_3$) δ 166.8, 132.9, 130.6, 130.5, 130.3, 129.5, 128.3, 72.9, 70.4, 70.4, 66.4, 65.0, 62.4, 29.2, 28.5, 22.7

To this diol (3.6 g, 9.9 mmol) in 30 mL of dry dichloromethane at 0 $^{\circ}$C under nitrogen, were added imidazole (1.0 g, 15 mmol) and TBSCl (1.6 g, 11 mmol). The reaction mixture stirred for 1 h at 0 $^{\circ}$C and was then diluted with 15 mL of water and extracted with dichloromethane (2 x 25 mL), the combined organic portionswas dried over Na$_2$SO$_4$ and the solvent was removed under reduced pressure. Then flash column chromatography with 20% EtOAc–cyclohexane, gave TBS protected intermediate (3.7 g, 78%) as a colourless syrup; TLC: R_f 0.3 in 20% EtOAc–cyclohexane; HRMS: [M+Na]$^+$ Calcd for $C_{24}H_{39}N_3O_5NaSi$ 500.2557, found 500.2556; ^{1}H NMR (500 MHz, CDCl$_3$) δ 8.07 – 8.01 (overlapped signals, 2H), 7.55 (t, J = 7.5 Hz, 1H), 7.43 (overlapped signals, 2H), 5.89 (dtd, J = 15.5, 5.4, 1.1 Hz, 1H), 5.77 (ddt, J = 15.5, 6.3, 1.4 Hz, 1H), 4.32 (overlapped signals, 2H), 4.28 (t, J = 5.3 Hz, 1H), 3.99 (overlapped signals, 2H), 3.86 – 3.79 (overlapped signals, 2H), 3.45 (overlapped signals, 2H), 3.41 (apparent q, J = 5.4 Hz, 1H), 2.529 (d, J = 5.2 Hz, 1H), 1.835 – 1.758 (overlapped signals, 2H), 1.654 (overlapped signals, 2H), 1.56 – 1.48 (overlapped signals, 2H), 0.90 (s, 9H), 0.086 (s, 6H); ^{13}C NMR (125 MHz, CDCl$_3$) δ 166.7, 132.8, 130.6, 130.3, 129.5, 128.3, 72.4, 70.5, 70.2, 66.1, 64.9, 63.5, 29.4, 28.6, 25.7, 22.7, 18.1, -5.6, -5.6.

To a stirred solution of this TBS protected intermediate (3.5 g, 7.3 mmol) in 30 mL of MeOH, was added K_2CO_3 (0.1 g, 0.7 mmol) at room temperature. The reaction mixture was stirred at room temperature for 2 h and then the solvent was removed under reduced pressure at room temperature, avoiding heating. Flash column chromatography with 50% EtOAc–cyclohexane, gave a primary alcohol intermediate (2.3 g, 86%) as a colourless syrup; TLC: R_f 0.2 in 60% EtOAc–cyclohexane; HRMS: $[M+Na]^+$ Calcd for $C_{17}H_{35}N_3O_4NaSi$ 396.2295, found 393.2291; ^1H NMR (500 MHz, CDCl$_3$) δ 5.89 (dt, $J = 15.7, 5.4$ Hz, 1H), 5.78 (dd, $J = 15.6, 6.3$ Hz, 1H), 4.29 (t, $J = 5.9$ Hz, 1H), 3.99 (overlapped signals, 2H), 3.83 (overlapped signals, 2H), 3.65 (overlapped signals, 2H), 3.45 (overlapped signals, 2H), 3.42 (d, $J = 5.8$ Hz, 1H), 1.61 (overlapped signals, 4H), 1.44 (overlapped signals, 2H), 0.91 (s, 9H), 0.09 (overlapped s, 6H); ^{13}C NMR (125 MHz, CDCl$_3$) δ 130.7, 130.3, 72.4, 70.5, 70.4, 66.1, 63.6, 62.8, 32.4, 29.4, 25.7, 22.4, 18.1-5.6.

To this primary alcohol (2.0 g, 5.3 mmol) in 30 mL of dry dichloromethane at 0 °C under nitrogen, were added imidazole (0.54 g, 8.0 mmol) and TBDPSCl (1.5 mL, 5.9 mmol). The reaction mixture was stirred for 2 h at 0 °C, then diluted with 15 mL of water, and extracted with dichloromethane (2x30 mL). The combined organic portions were dried over Na_2SO_4 and the solvent was removed under reduced pressure. Flash column chromatography with 10% EtOAc–cyclohexane, gave the TBDPS protected intermediate (2.8 g, 86%) as a colourless syrup; TLC: R_f 0.2 in 10% EtOAc–cyclohexane; HRMS: $[M+Na]^+$ Calcd for $C_{33}H_{53}N_3O_4NaSi_2$ 634.3472, found 634.3475; ^1H NMR (500 MHz, CDCl$_3$) δ 7.69 – 7.64 (overlapped signals, 4H), 7.44 – 7.35 (overlapped signals, 6H), 5.89 (dt, $J = 15.4, 5.4$ Hz, 1H), 5.77 (dd, $J = 15.5, 6.4$ Hz, 1H), 4.29 (apparent q, $J = 5.7$ Hz, 1H), 3.98 (overlapped signals, 2H), 3.87 – 3.78 (overlapped signals, 2H), 3.66 (overlapped signals, 2H), 3.41 (overlapped signals, 3H), 2.42 (d, $J = 5.3$ Hz, 1H), 1.62 – 1.56 (overlapped signals, 4H), 1.41 (overlapped signals, 2H), 1.04 (s, 9H), 0.91 (s, 9H), 0.09 (overlapped s, 6H); ^{13}C NMR (125 MHz, CDCl$_3$) δ 135.5, 134.1, 130.4, 130.4, 129.5, 127.6, 72.5, 70.6, 70.4, 66.0, 63.8, 63.6, 32.4, 29.5, 26.9, 25.7, 22.4, 19.2, 18.1, -5.6, -5.6.

To this TBDPS protected intermediate, which had a secondary alcohol (2.5 g, 4.1 mmol), in 40 mL of dry dichloromethane at 0 °C under nitrogen, were added 5 mL pyridine and, slowly, benzoyl chloride (0.94 mL, 8.2 mmol). The mixture was stirred for 2 h at room temperature, then diluted with 20 mL of sat aq $NaHCO_3$, and extracted with dichloromethane (2 x 30 mL), the combined organic portions dried over Na_2SO_4 and the solvent was removed under reduced pressure. Flash column chromatography with

5% EtOAc–cyclohexane gave a benzoylated intermediate (2.6 g, 91%) as a colourless syrup; TLC: R_f 0.5 in 10% EtOAc–cyclohexane; HRMS: [M+Na]$^+$ Calcd for $C_{40}H_{57}N_3O_5NaSi_2$ 738.3734, found 738.3712; ^{1}H NMR (500 MHz, CDCl$_3$) δ 8.05 (overlapped signals, 2H), 7.65 (overlapped signals, 4H), 7.61 – 7.52 (m, 1H), 7.47 – 7.42 (overlapped signals, 2H), 7.41 – 7.33 (overlapped signals, 5H), 7.30 – 7.09 (m, 1H), 6.01 – 5.93 (m, 1H), 5.86 – 5.79 (m, 1H), 5.68 (t, J = 5.7 Hz, 1H), 3.99 (overlapped signals, 2H), 3.84 – 3.77 (m, 1H), 3.73 (overlapped signals, 2H), 3.68 – 3.60 (overlapped signals, 2H), 3.39 (overlapped signals, 2H), 1.62 – 1.56 (overlapped signals, 4H), 1.40 (overlapped signals, 2H), 1.03 (s, 9H), 0.90 (s, 9H), 0.06 (overlapped signals, 6H); ^{13}C NMR (125 MHz, CDCl$_3$) δ 165.1, 135.5, 134.1, 133.3, 133.2, 129.7, 129.5, 128.4, 127.6, 125.2, 73.4, 70.6, 70.2, 65.6, 63.8, 62.8, 32.4, 29.4, 26.8, 25.7, 22.3, 19.2, 18.1, -5.6, -5.6.

To this benzoylated intermediate (4 g, 5.6 mmol) in 120 mL of THF, was added 1M HCl (5.6 mL, 5.6 mmol). The reaction mixture was stirred for 48 h and was then 10 mL of triethylamine was added. Then the volatile components were removed under reduced pressure, while not heating above room temperatura (20 C). Column chromatography with 1:19 EtOAc–cyclohexane gave the recovered unreacted intermediate (1 g); subsequent elution with 30:70 EtOAc–cyclohexane gave **13** (2.0 g, 81%) as a syrup; TLC: R_f 0.2 in 30:70 EtOAc–cyclohexane; HRMS: [M+Na]$^+$ Calcd for $C_{34}H_{43}N_3O_5NaSi$ 624.2870, found 624.2886; ^{1}H NMR (500 MHz, CDCl$_3$) δ 8.09 – 8.03 (overlapped signals, 2H), 7.69 – 7.63 (overlapped signals, 4H), 7.49 – 7.33 (overlapped signals, 8H), 6.02 (dt, J = 15.6, 5.1 Hz, 1H), 5.88 (ddt, J = 15.5, 7.3, 1.7 Hz, 1H), 5.71 (dd, J = 7.2, 5.0 Hz, 1H), 4.03 – 3.96 (overlapped signals, 2H), 3.83 (dt, J = 6.9, 4.5 Hz, 1H), 3.78 (ddd, J = 11.7, 7.5, 4.2 Hz, 1H), 3.71 – 3.62 (overlapped signals, 3H), 3.41 (t, J = 6.6 Hz, 2H), 2.15 – 2.05 (m, 1H), 1.62 – 1.52 (overlapped signals, 4H), 1.43 – 1.36 (overlapped signals, 2H), 1.04 (s, 9H); ^{13}C NMR (125 MHz, CDCl$_3$) δ 165.4, 135.5, 134.1, 133.6, 133.4, 129.8, 129.5, 128.5, 127.6, 125.0, 73.7, 70.7, 70.1, 66.0, 63.8, 61.8, 32.3, 29.4, 26.9, 26.9, 22.3, 19.2.

Preparation of 14 To stirred **6** (3.7 g, 5.0 mmol) and **13** (2 g, 3.3 mmol) in 40 mL dry dichloromethane at 0 °C under nitrogen, was added slowly, BF$_3$.Et$_2$O (0.6 mL, 5.0 mmol) in 3 mL of dry dichloromethane, and the mixture stirred for 1 h at 0 °C. Then it was diluted with 20 mL of sat aq NaHCO$_3$, and extracted with dichloromethane (2 x 30 mL). The combined organic portions were dried over Na$_2$SO$_4$, the solvent was removed under reduced pressure and flash column chromatography of the residue with 18:82 EtOAc–cyclohexane, gave **14** (3.2 g, 83%) as a white solid; TLC: R_f 0.6 in 50:50 EtOAc–cyclohexane; HRMS: [M+Na]$^+$ Calcd for $C_{68}H_{69}N_3O_{14}NaSi$ 1202.4447, found 1202.4420; ^{1}H

NMR (500 MHz, CDCl$_3$) δ 8.15 – 8.09 (overlapped signals, 2H), 8.07 – 7.95 (overlapped signals, 6H), 7.80 (dd, J = 8.3, 1.4 Hz, 2H), 7.70 – 7.64 (overlapped signals, 4H), 7.65 – 7.60 (m, 1H), 7.58 – 7.47 (overlapped signals, 4H), 7.46 – 7.34 (overlapped signals, 13H), 7.28 – 7.22 (overlapped signals, 2H), 6.01 (dd, J = 3.5, 1.1 Hz, 1H), 5.89 – 5.82 (overlapped signals, 2H), 5.82 – 5.75 (m, 1H), 5.71 (dd, J = 6.9, 4.4 Hz, 1H), 5.63 (dd, J = 10.4, 3.4 Hz, 1H), 4.90 (d, J = 7.9 Hz, 1H), 4.62 (dd, J = 11.0, 6.2 Hz, 1H), 4.39 (t, J = 5.5 Hz, 1H), 4.36 – 4.30 (m, 1H), 4.09 (dd, J = 10.2, 6.7 Hz, 1H), 4.05 – 3.98 (m, 1H), 3.92 – 3.81 (overlapped signals, 2H), 3.76 (dd, J = 10.2, 5.4 Hz, 1H), 3.66 (overlapped signals, 2H), 3.34 (overlapped signals, 2H), 1.55 (overlapped signals, 4H), 1.43 – 1.34 (overlapped signals, 2H), 1.05 (s, 9H); ^{13}C NMR (125 MHz, CDCl$_3$) δ 166.0, 165.6, 165.5, 165.1, 164.9, 135.6, 134.1, 133.8, 133.6, 133.3, 133.2, 133.2, 130.1, 129.8, 129.8, 129.8, 129.7, 129.5, 129.4, 129.3, 129.0, 128.7, 128.7, 128.5, 128.4, 128.4, 128.3, 127.6, 124.5, 101.2, 73.7, 71.6, 71.4, 70.7, 70.0, 69.6, 68.1, 67.9, 63.8, 63.4, 61.9, 32.4, 29.4, 26.9, 26.9, 22.3, 19.2.

Preparation of 15   To stirred **14** (2.8 g, 2.3 mmol) in 60 mL of 1:5 THF-H$_2$O, was added PPh$_3$ (1.9 g, 7.1 mmol). The reaction mixture was stirred for 14 h at 40 °C, then diluted with 10 mL of sat aq NaCl, and extracted with EtOAc (2 x 30 mL). The combined organic portions were dried over Na$_2$SO$_4$ and the solvent was removed under reduced pressure and the residue used in the next step without further purification.   Thus, to the residue were added butyric acid (0.3 mL, 3.6 mmol) in 25 mL MeCN, DIPEA (3 mL) and EDCI (1.9 mL, 10.8 mmol). The mixture was stirred for 2 h at room temperature, then diluted with 10 mL of sat aq NaHCO$_3$, and extracted with EtOAc (2 x 30 mL). The combined organic portions were dried over Na$_2$SO$_4$ and the solvent was removed under reduced pressure. Flash chromatography of the residue with 22:78 EtOAc–cyclohexane gave **15** (1.8 g, 61%) as a white solid; TLC: R_f 0.5 in 50% EtOAc–cyclohexane; HRMS: [M+Na]$^+$ Calcd for C$_{72}$H$_{77}$NO$_{15}$NaSi 1246.4960, found 1246.4962; ^{1}H NMR (500 MHz, CDCl$_3$) δ 8.16 – 8.10 (overlapped signals, 2H), 8.06 – 8.01 (overlapped signals, 2H), 7.95 (overlapped signals, 4H), 7.81 – 7.75 (overlapped signals, 2H), 7.69 – 7.61 (overlapped signals, 5H), 7.57 – 7.47 (overlapped signals, 5H), 7.46 – 7.34 (overlapped signals, 13H), 7.29 – 7.22 (overlapped signals, 2H), 6.00 – 5.89 (overlapped signals, 2H), 5.84 – 5.72 (overlapped signals, 3H), 5.70 (t, J = 7.0 Hz, 1H), 5.64 (ddd, J = 10.4, 3.6, 1.6 Hz, 1H), 4.79 (dd, J = 7.8, 1.7 Hz, 1H), 4.59 – 4.50 (m, 1H), 4.34 (ddd, J = 10.8, 6.0, 1.7 Hz, 1H), 4.29 (dt, J = 9.5, 2.0 Hz, 1H), 4.25 (t, J = 6.4 Hz, 1H), 4.19 (ddd, J = 10.9, 6.7, 1.7 Hz, 1H), 3.94 (d, J = 5.6 Hz, 2H), 3.73 – 3.68 (m, 1H), 3.65 (overlapped signals, 2H), 3.41 – 3.30 (overlapped signals, 2H), 1.82 (overlapped signals, 2H), 1.55 (overlapped signals, 4H), 1.48 – 1.44 (m, 1H), 1.42 – 1.34 (overlapped signals, 3H), 1.04

(overlapped signals, 9H), 0.75 (m, 3H); ^{13}C NMR (125 MHz, CDCl$_3$) δ 172.6, 165.8, 165.5, 165.5, 165.4, 165.1, 134.1, 133.7, 133.5, 133.3, 133.3, 133.1, 132.4, 130.1, 130.1, 129.8, 129.7, 129.6, 129.5, 129.3, 129.1, 129.0, 128.7, 128.6, 128.5, 128.4, 128.3, 1276, 127.2, 101.0, 73.2, 71.3, 70.5, 70.5, 70.2, 67.9, 67.4, 63.8, 61.6, 50.6, 38.3, 32.4, 29.4, 26.9, 26.9, 22.3, 19.2, 18.9, 13.6.

Preparation of 16   To stirred **15** (1.4 g, 1.1 mmol) in 30 mL of 1:1 dichloromethane-MeOH, was added *p*TSA (0.2 g, 1.1 mmol) and the mixture was stirred for 16 h at room temperature. Then the mixture was diluted with 15 mL of sat aq NaHCO$_3$ and extracted with EtOAc (2 x 25 mL).   The combined organic portions were dried over Na$_2$SO$_4$ and the solvent was removed under reduced pressure. Flash column chromatography with 80% EtOAc–cyclohexane, gave the primary alcohol intermediate (0.97 g, 86%) as a white solid; TLC: R_f 0.3 in 80:20 EtOAc–cyclohexane; HRMS: [M+Na]$^+$ Calcd for C$_{56}$H$_{59}$NO$_{15}$Na 1008.3782, found 1008.3765; ^{1}H NMR (500 MHz, CDCl$_3$) δ 8.12 (overlapped signals, 2H), 8.03 (overlapped signals, 2H), 7.94 (overlapped signals, 4H), 7.77 (overlapped signals, 2H), 7.64 (dd, J = 8.4, 6.6 Hz, 1H), 7.51 (overlapped signals, 5H), 7.45 – 7.32 (overlapped signals, 7H), 7.28 – 7.20 (overlapped signals, 2H), 5.99 – 5.90 (overlapped signals, 3H), 5.87 – 5.77 (m, 1H), 5.74 (ddd, J = 9.8, 7.7, 1.8 Hz, 1H), 5.69 (t, J = 7.2 Hz, 1H), 5.66 – 5.60 (m, 1H), 4.80 (dd, J = 7.9, 1.8 Hz, 1H), 4.56 (m, 1H), 4.30 (overlapped signals, 2H), 4.24 (t, J = 6.4 Hz, 1H), 4.16 (ddd, J = 10.9, 6.6, 1.8 Hz, 1H), 3.99 – 3.89 (overlapped signals, 2H), 3.70 (dt, J = 9.8, 2.5 Hz, 1H), 3.61 (overlapped signals, 2H), 3.39 (overlapped signals, 2H), 1.90 – 1.78 (overlapped signals, 2H), 1.63 – 1.51 (overlapped signals, 4H), 1.43 (overlapped signals, 4H), 0.75 (m, 3H); ^{13}C NMR (125 MHz, CDCl$_3$) δ 172.7, 165.8, 165.5, 165.5, 165.5, 165.1, 133.7, 133.6, 133.3, 133.3, 133.1, 132.4, 130.1, 130.1, 129.7, 129.7, 129.6, 129.3, 129.0, 129.0, 128.7, 128.7, 128.6, 128.5, 128.4, 128.3, 127.1, 100.9, 73.1, 71.3, 71.3, 70.3, 70.2, 67.9, 67.3, 62.6, 61.6, 50.6, 38.3, 32.4, 29.3, 22.5, 18.9, 13.5. To this intermediate (1.5 g, 1.5 mmol) in 25 mL of dry dichloromethane, was added 3 mL of triethylamine and MsCl (0.35 mL, 4.5 mmol) and the mixture was stirred for 30 min at room temperature. It was then diluted with 10 mL of sat aq NaHCO$_3$, and extracted with dichloromethane (2 x 20 mL), the combined organic portions were dried over Na$_2$SO$_4$ and the solvent was removed under reduced pressure. The residue, used without further purification, was taken up in 15 mL dry DMF, NaN$_3$ (0.29 mg, 4.5 mmol) was added and then the reaction mixture was stirred at 80 °C for 3 h. It was then diluted with 50 mL of H$_2$O, and extracted with EtOAc (3 x 20 mL) and the combined organic portions were dried over Na$_2$SO$_4$. The solvent was removed under reduced pressure and flash column chromatography of the residue with 25:75 EtOAc–cyclohexane, gave **16** (1.2 g, 78%) as a white solid; TLC: R_f 0.2 in 20:80 EtOAc–cyclohexane; HRMS: [M+Na]$^+$ Calcd for

C$_{56}$H$_{58}$N$_4$O$_{14}$Na 1033.3847, found 1033.3883; ^{1}H NMR (500 MHz, CDCl$_3$) δ 8.15 – 8.10 (overlapped signals, 2H), 8.06 – 8.01 (overlapped signals, 2H), 7.98 – 7.92 (overlapped signals, 4H), 7.80 – 7.75 (overlapped signals, 2H), 7.68 – 7.61 (m, 1H), 7.52 (overlapped signals, 5H), 7.45 – 7.34 (overlapped signals, 7H), 7.24 (overlapped signals, 2H), 5.94 (overlapped signals, 2H), 5.84 – 5.77 (overlapped signals, 2H), 5.74 (dd, J = 10.4, 7.7 Hz, 1H), 5.69 (t, J = 6.9 Hz, 1H), 5.64 (dd, J = 10.4, 3.4 Hz, 1H), 4.80 (d, J = 7.8 Hz, 1H), 4.55 (ddt, J = 10.3, 7.0, 3.3 Hz, 1H), 4.33 (dd, J = 10.9, 6.1 Hz, 1H), 4.29 (dd, J = 9.6, 3.1 Hz, 1H), 4.25 (t, J = 6.4 Hz, 1H), 4.18 (dd, J = 10.9, 6.6 Hz, 1H), 3.95 (overlapped signals, 2H), 3.70 (dd, J = 9.6, 3.7 Hz, 1H), 3.38 (overlapped signals, 2H), 3.23 (overlapped signals, 2H), 1.89 – 1.76 (overlapped signals, 2H), 1.58 (overlapped signals, 4H), 1.50 – 1.43 (overlapped signals, 2H), 1.41 – 1.36 (overlapped signals, 2H), 1.27 (overlapped signals, 3H), 0.76 (m, 3H); ^{13}C NMR (125 MHz, CDCl$_3$) δ 172.6, 165.8, 165.5, 165.5, 165.4, 165.1, 133.7, 133.6, 133.3, 133.3, 133.1, 132.2, 130.1, 130.1, 129.7, 129.7, 129.6, 129.3, 129.1, 129.0, 128.7, 128.6, 128.4, 128.4, 128.3, 127.3, 101.0, 73.2, 71.3, 70.4, 70.2, 70.1, 67.9, 67.3, 61.6, 51.3, 50.5, 38.3, 29.2, 28.7, 26.9, 23.4, 18.9, 13.6.

Preparation of clickable sulfatide-2 To the stirred azide **16** (1.0 g, 0.99 mmol) in 15 mL of 1:1 MeOH–dichloromethane, was added K$_2$CO$_3$ (0.14 g, 0.99 mmol). The reaction mixture was stirred for 16 h, at room temperature. The solvent was removed under reduced pressure and flash chromatography using 16:84 MeOH–dichloromethane as eluant, gave the penta-ol intermediate (0.44 g, 91%) as a white solid; TLC: R_f 0.1 in 15% MeOH–dichloromethane; HRMS [M+Na]$^+$ Calcd for C$_{21}$H$_{38}$N$_4$O$_9$Na 513.2536, found 513.2516; ^{1}H NMR (500 MHz, CD$_3$OD) δ 5.79 (dt, J = 15.6, 5.1 Hz, 1H), 5.73 (dd, J = 15.7, 6.1 Hz, 1H), 4.27 – 4.18 (overlapped signals, 2H), 4.16 (dd, J = 10.2, 5.0 Hz, 1H), 4.02 (dt, J = 8.1, 4.2 Hz, 1H), 3.95 (overlapped signals, 2H), 3.83 (d, J = 3.3 Hz, 1H), 3.76 (dd, J = 11.3, 7.0 Hz, 1H), 3.72 (dd, J = 11.3, 5.1 Hz, 1H), 3.62 (dd, J = 10.3, 3.5 Hz, 1H), 3.57 – 3.50 (overlapped signals, 2H), 3.47 (dd, J = 3.5, 1.3 Hz, 1H), 3.44 (overlapped signals, 2H), 3.29 (overlapped signals, 2H), 2.17 (overlapped signals, 2H), 1.61 (overlapped signals, 6H), 1.44 (overlapped signals, 2H), 0.94 (m, 3H); ^{13}C NMR (125 MHz, CD$_3$OD) δ 174.6, 132.5, 128.9, 103.9, 75.3, 73.4, 71.2, 70.9, 70.4, 69.7, 68.9, 68.4, 61.1, 53.4, 51.0, 37.8, 28.9, 28.3, 23.1, 19.0, 12.7. To the stirred penta-ol (0.4 g, 0.8 mmol) in 15 mL dry MeOH, was added Bu$_2$SnO (0.3 g, 1.2 mmol) and the mixture was heated at 60°C for 2 h. Then the solvent was removed under reduced pressure and was dried under high vacuum for 30 mins. When the residue was well dried, it was taken up in 15 mL dry THF, and then SO$_3$.NEt$_3$ (0.22 g, 1.6 mmol) was added. The reaction mixture was stirred for 16 h at room temperature. Then the solvent was removed under reduced pressure and the residue was dissolved in 20 mL of 1:1 MeOH–dichloromethane and

passed through a small bed of Na$^+$ resin. The solvent was then removed under reduced pressure and flash column chromatography with 18% MeOH–dichloromethane gave the **clickable sulfatide-2** (0.42 g, 89% 3 steps) as a white solid; TLC: R_f 0.2 in 20% MeOH–dichloromethane; HRMS [M+Na]$^+$ Calcd for $C_{21}H_{37}N_4O_{12}Na_2S$ 615.1924, found 615.1907; ^{1}H NMR (500 MHz, CD$_3$OD) δ 5.79 (dt, J = 15.6, 5.2 Hz, 1H), 5.73 (dd, J = 15.6, 6.3 Hz, 1H), 4.34 (d, J = 7.7 Hz, 1H), 4.27 – 4.16 (overlapped signals, 4H), 4.01 (dt, J = 7.9, 3.9 Hz, 1H), 3.95 (overlapped signals, 2H), 3.79 – 3.70 (overlapped signals, 3H), 3.62 (dd, J = 10.3, 3.4 Hz, 1H), 3.57 (t, J = 6.0 Hz, 1H), 3.43 (overlapped signals, 2H), 3.28 (overlapped signals, 2H), 2.17 (overlapped signals, 2H), 1.61 (overlapped signals, 6H), 1.50 – 1.39 (overlapped signals, 2H), 0.94 (m, 3H); ^{13}C NMR (125 MHz, CD$_3$OD) δ 174.6, 132.5, 128.9, 103.7, 80.3, 75.0, 70.8, 70.4, 69.7, 69.5, 68.4, 67.1, 61.0, 53.3, 51.0, 37.7, 28.9, 28.3, 23.1, 19.0, 12.7.

General Experimental for JGD Synthesis

All reagents were obtained from commercial sources and used without purification unless otherwise stated. THF was distilled over Na/benzophenone immediately before use. ^{1}H and ^{13}C NMR spectra were recorded at 500 MHz and 126 MHz respectively, on a Bruker DRX (500 MHz) NMR spectrometer. All NMR spectra were measured at 23 °C. Chemical shifts (δ) are reported in ppm and coupling constants (J) are reported in Hertz (Hz). The resonance multiplicities in the ^{1}H NMR spectra are described as "s" (singlet), "d" (doublet), "t" (triplet), and "m" (multiplet) and broad resonances are indicated by "br". Residual protic solvent of CDCl$_3$ (^{1}H, δ 7.26 ppm; ^{13}C, δ 77.16 ppm), and tetramethylsilane (TMS, δ 0 ppm) were used as the internal reference in the ^{1}H- and ^{13}C-NMR spectra. The absorptions are given in wavenumbers (cm^{-1}). Progress of the reaction was monitored by thin-layer chromatography (TLC) using silica gel 60 F$_{254}$ precoated plates (E. Merck) and compounds were visualized by UV light with a wavelength of 254 nm. Purifications by flash column chromatography were performed using flash silica gel from Silicycle (60 Å, 40–63 μm) with the indicated eluent. The purity of the products was determined by a combination of TLC and high-pressure liquid chromatography (HPLC) was carried out using Shimadzu LC-20AD high-performance liquid chromatograph pump, a PE Nelson Analytical 900 Series integration data station, a Shimadzu SPD-10A VP (UV-*vis*, λ = 254 nm) and three AM gel columns (a guard column, two 500 Å, 10 μm columns). THF was used as solvent at the oven temperature of 23 ºC. Detection was done by UV absorbance at 254 nm. MALDI-TOF mass spectrometry was performed on a PerSeptive Biosystem-Voyager-DE (Framingham, MA) MALDI-TOF

mass spectrometer equipped with nitrogen laser (337 nm) and operating in linear mode. Internal calibration was performed using angiotensin II and bombesin as standards. The analytical sample was obtained by mixing the THF solution of the sample (5–10 mg/mL) and THF solution of the matrix (2,5-dihydroxybenzoic acid, 10 mg/mL) in a 1/5 (v/v) ratio. The prepared solution of the sample and the matrix (0.5 μL) was loaded on the MALDI plate and allowed to dry at 23 ºC before the plate was inserted into the vacuum chamber of the MALDI instrument. The laser steps and voltages applied were adjusted depending on both the molecular weight and the nature of each analyzed compound.

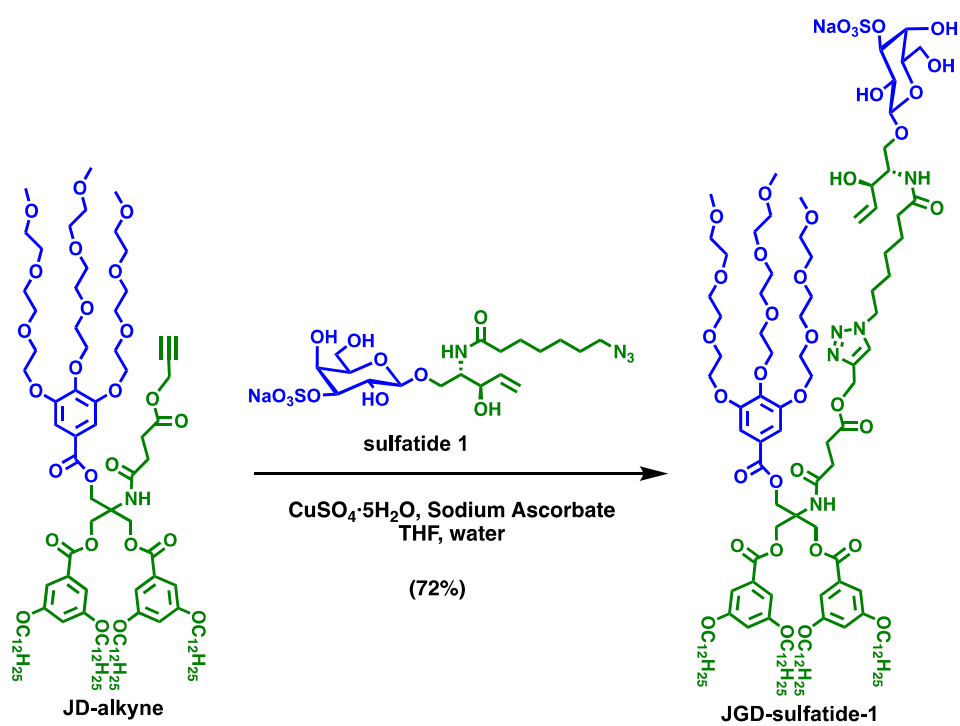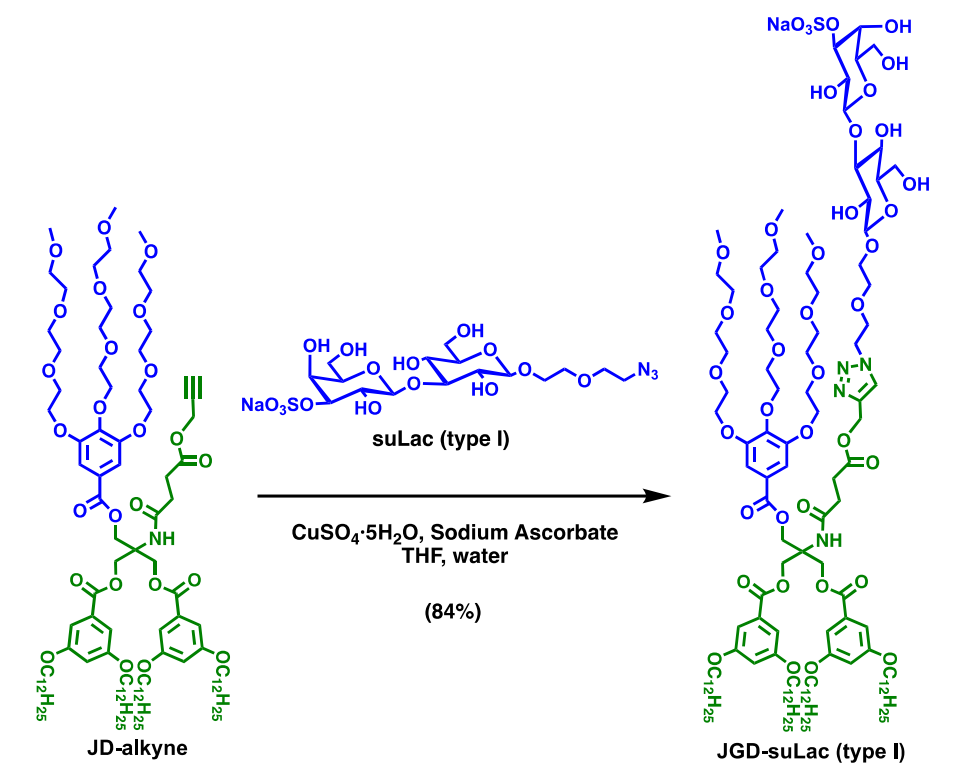## Synthesis of JD-A and Lac/Man-presenting GDSs

2-(3,4,5-Tris(((methyl triethylene glycol)benzoyl)oxy))-2,2-bis-hydroxymethyl-3-oxo-prop2-yn-1-yl succinate (**JD-alkyne)**, Janus dendrimer **JGD-Lac** and **JGD-Man** were synthesized and characterized as described before (Percec et al., 2013; Zhang et al., 2014).
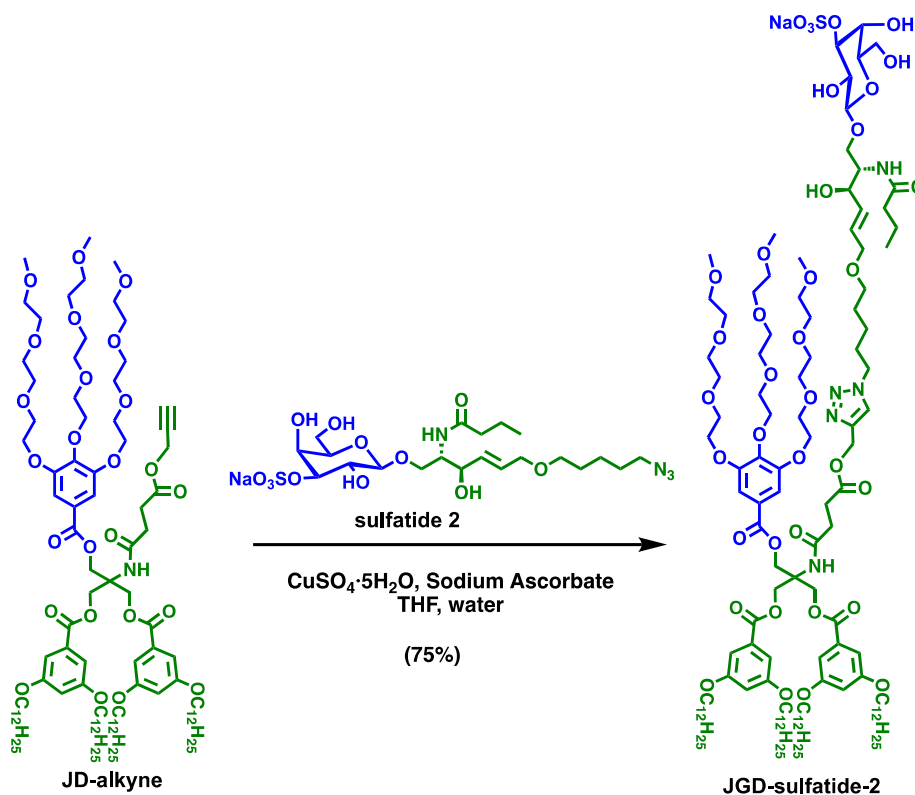
JGD-suLac (type I). To a mixed solution of **JD-alkyne** (Kabsch, 2010) (see SI, 200 mg, 0.114 mmol) in THF (13 mL) and **suLac (type I)** (61 mg, 0.114 mmol) in water (2 mL) was added $CuSO_4 \cdot 5H_2O$ (28 mg, 0.182 mmol) in water (2 mL), and sodium ascorbate (45 mg, 0.228 mmol) in water (2 mL), successively, under nitrogen atmosphere. The reaction mixture was allowed to stir at 23 °C for 24 h. The reaction mixture was concentrated to dryness. The crude product was further purified by silica column chromatography with a mobile phase of CH_2Cl_2-MeOH, 10:1 to 5:1 to yield compound **JGD-suLac (type I)** (sodium salt) as a light-yellow gel (220 mg, 84%). Purity (HPLC): 99%+. ^{1}H NMR (500 MHz, CDCl$_3$) δ = 7.75 (s, 1H, 1×=*CH* (triazole)), 7.35 (s, 2H, 2×Ar*H*), 7.07 (s, 4H, 4×Ar*H*), 6.59 (s, 2H, 2×Ar*H*), 5.14 (m, 2H), 4.81–4.86 (m, 6H), 4.55 (m, 2H), 4.27 (m, 8H), 3.52–3.89 (m, 42H), 3.37 (m, 9H, 3×O*CH₃*), 2.61–2.65 (m, 4H), 1.72–1.74 (m, 8H, 4×-ArCH$_2$*CH₂*CH$_2$(CH$_2$)$_8$CH$_3$), 1.40–1.41 (m, 8H, 4×-ArCH$_2$CH$_2$*CH₂*(CH$_2$)$_8$CH$_3$), 1.25– (m, 64H, 4×-ArCH$_2$CH$_2$CH$_2$*(CH₂)₈*CH$_3$), 0.85–0.88 (t, *J* = 6.9 Hz, 12H, 4×-Ar(CH$_2$)$_{11}$*CH₃*). ^{13}C NMR (126 MHz, CDCl$_3$) δ = 172.6, 172.3, 165.9, 165.7, 160.1, 152.1, 142.2, 131.0, 124.4, 109.0, 107.7, 106.5, 103.8, 102.4, 79.7, 75.6, 74.7, 72.3, 71.8, 70.5, 70.4, 70.4, 70.3, 69.4, 68.7, 68.2, 63.9, 61.3, 58.9, 58.8, 57.8, 50.3, 32.6, 31.7, 31.0, 29.4, 29.2, 26.0, 23.0, 22.8, 22.5, 13.6. MALDI-TOF (m/z): [M+Na]$^+$ cald. for C$_{117}$H$_{195}$N$_4$ Na$_2$O$_{40}$S: 2374.29; found 2372.80.

JGD-sulfatide-1. To a mixed solution of **JD-alkyne** (see SI, 200 mg, 0.114 mmol) in THF (13 mL) and **sulfatide-1** (61 mg, 0.114 mmol) in water (2 mL) was added $CuSO_4 \cdot 5H_2O$ (28 mg, 0.114 mmol) in

water (2 mL), and sodium ascorbate (45 mg, 0.228 mmol) in water (2 mL), successively, under nitrogen atmosphere. The reaction mixture was allowed to stir at 23 °C for 24 h. The reaction mixture was concentrated to dryness. The crude product was further purified by silica column chromatography with a mobile phase of CH_2Cl_2/MeOH, 10:1 to 5:1 to yield compound **JGD-sulfatide-1** (sodium salt) as a light yellow gel 190 mg, 72%). Purity (HPLC): 99%+. ^{1}H NMR (500 MHz, CDCl$_3$) δ = 7.75 (s, 1H, 1×C*H* (triazole)), 7.33 (s, 2H, 2×Ar*H*), 7.07 (s, 4H, 4×Ar*H*), 6.59 (s, 2H, 2×Ar*H*), 5.84 (m, 1H, 1×C*H*=), 5.28 (m, 1H, 1×C*H*=), 5.14 (m, 3H, 1×O-*CH$_2$*-TRZ and 1×C*H*=), 4.84 (m, 6H, 3×*CH$_2$*), 4.32–4.32 (m, 10H), 4.04 (m, 2H), 3.52–3.89 (m, 46H), 3.35–3.36 (m, 9H, 3×O*CH$_3$*), 2.65 (br, 2H, 1×COO-*CH$_2$*CH$_2$CONH), 2.58 (br, 2H, COO-CH$_2$*CH$_2$*CONH), 1.86 (m, 2H), 1.72–1.75 (m, 8H), 1.56 (m, 2H), 1.44 (m, 8H), 1.25–1.30 (m, 72H), 0.85–0.88 (t, 12H). ^{13}C NMR (126 MHz, CDCl$_3$) δ = 174.4, 172.6, 172.2, 166.0, 165.7, 160.4, 160.1, 152.1, 142.2, 137.3, 131.0, 124.5, 116.3, 109.0, 107.8, 106.6, 103.3, 80.0, 74.1, 72.3, 71.8, 70.4, 70.3, 69.4, 68.7, 68.3, 67.2, 63.8, 60.7, 59.4, 59.0, 58.9, 53.3, 50.8, 36.2, 36.1, 32.0, 31.8, 31.1, 29.7, 29.6, 29.6, 29.4, 29.3, 29.2, 28.3, 26.0, 25.9, 25.4, 14.1. MALDI-TOF (m/z): [M+Na]$^+$ cald. for $C_{119}H_{198}N_5Na_2O_{36}S$: 2351.33; found 2353.6.

JGD-sulfatide-2. To a mixed solution of **JD-alkyne** (see SI, 200 mg, 0.114 mmol) in THF (13 mL) and **sulfatide-2** (61 mg, 0.114 mmol) in water (2 mL) was added CuSO$_4$·5H$_2$O (28 mg, 0.114 mmol) in water (2 mL), and sodium ascorbate (45 mg, 0.228 mmol) in water (2 mL), successively, under nitrogen atmosphere. The reaction mixture was allowed to stir at 23 °C for 24 h. The reaction mixture was concentrated to dryness. The crude product was further purified by silica column chromatography with a mobile phase of CH_2Cl_2/MeOH, 10:1 to 5:1 to yield compound **JGD-sulfatide-2** (sodium salt) as a light yellow gel (207 mg, 75%). Purity (HPLC): 99%+. ^{1}H NMR (500 MHz, CDCl$_3$) δ = 7.71 (s, 1H, 1×C*H* (triazole)), 7.31 (s, 2H, 2×Ar*H*), 7.08 (s, 4H, 4×Ar*H*), 6.59 (s, 2H, 2×Ar*H*), 5.74–5.78 (m, 2H, 1×C*H$_2$*=), 5.13 (m, 3H, 1×O-*CH$_2$*-TRZ), 4.80–4.84 (m, 6H, 3×*CH$_2$*), 4.22–4.33 (m, 12H), 4.10 (m, 2H), 3.52–3.89 (m, 50H), 3.35–3.36 (m, 12H), 2.65 (br, 2H, 1×COO-*CH$_2$*CH$_2$CONH), 2.57 (br, 2H, COO-CH$_2$*CH$_2$*CONH), 2.16 (m, 2H), 2.04 (m, 6H), 1.91 (m, 2H), 1.72–1.75 (m, 8H), 1.58 (m, 4H), 1.39–1.42 (m, 8H), 1.25 (m, 70H), 0.85–0.88 (m, 15H). ^{13}C NMR (126 MHz, CDCl$_3$) δ = 174.3, 172.5, 172.1, 166.0, 165.7, 160.2, 160.2, 152.2, 142.3, 131.2, 129.0, 124.4, 109.1, 107.8, 106.6, 103.4, 79.9, 73.9, 72.3, 71.8, 71.7, 70.5, 70.4, 69.9, 69.4, 68.7, 68.3, 63.8, 59.0, 53.3, 50.4, 38.3, 31.9, 31.3, 30.0, 29.7, 29.6, 29.6, 29.4, 29.3, 29.2, 29.0, 26.0, 23.3, 22.7, 19.2, 14.1, 13.8. MALDI-TOF (m/z): [M+Na]$^+$ cald. for $C_{122}H_{204}N_5Na_2O_{37}S$: 2409.38; found 2410.05.

JD-alkyne

suLac (type I)

CuSO$_4$·5H$_2$O, Sodium Ascorbate
THF, water

(84%)

JGD-suLac (type I)

JD-alkyne

sulfatide 1

CuSO$_4$·5H$_2$O, Sodium Ascorbate
THF, water

(72%)

JGD-sulfatide-1

JD-alkyne → **JGD-sulfatide-2**

sulfatide 2

CuSO$_4$·5H$_2$O, Sodium Ascorbate
THF, water

(75%)

Preparation of nanoscale GDSs in injection method

A stock solution was prepared by dissolving the required amount of amphiphilic Janus glycodendrimers in ethanol. GDSs were then generated by injection of 100 μL of the stock solution into 2.0 mL PBS, followed by 5 sec vortexing.

Dynamic light scattering

DLS measurements of nanoscale GDSs were performed with a Malvern Zetasizer Nano-S instrument equipped with 4 mW He-Ne laser (633 nm) and avalanche photodiode positioned at 175° to the beam. Instrument parameters and measurement times were determined automatically. Experiments were performed in triplicate.

Aggregation assays

Aggregation assays of nanoscale GDSs with lectins were performed in semimicro disposable cuvettes at 23 °C and the course of OD was monitored at the wavelength $\lambda = 450$ nm by using a Shimadzu UV-vis spectrophotometer UV-1601 with Shimadzu/UV Probe software in kinetic mode. PBS containing

galectin (100 μL) was injected into PBS solution of GDSs (900 μL). The cuvette was shaken by hand for 1–2 s before data collection was started. The same solution of GDSs solution was used as a reference. PBS solutions of galectin were prepared before the aggregation assays and were maintained at 0 °C (ice bath) before data collection.

Cloning and expression of galectins

Generation of cDNAs and recombinant expression of galectins-1, -2, -4 (wild type, linker variants and domains), -8S and -3 and its 8S-linked homodimer were described previously (André et al., 2014; Kopitz et al., 2010, 2012; Ludwig et al., 2019; Saal et al., 2005; Xiao et al., 2018). To produce the Gal-4CC variant, full-length cDNA for two directly linked CRDs was obtained by applying a two-step PCR procedure previously described for Gal-1.[S15] In the first step, two DNA fragments were generated using the sense primer 5' gctcatatgcctgtgccatatttcgggagg '3 and the antisense primer 5' cctcccgaaatatggcacagggatctggacataggacaaggtg'3 to amplify the first fragment (the N-terminal Gal-4C domain) and the sense primer 5' caccttgtcctatgtccagatccctgtgccatatttcgggagg '3 and the antisense primer 5' cgaaagcttttagatctggacataggacaaggtg '3 for the second domain (C-terminal Gal-4C domain). In the second step, these PCR-products were used as a template to produce full-length cDNA for Gal-4CC with the sense primer 5' gctcatatgcctgtgccatatttcgggagg '3 (internal restriction site for *Nde*I underlined) and the antisense primer 5' cgaaagcttttagatctggacataggacaaggtg '3 (internal restriction site for *Hind*III underlined). In-frame ligation into the pGEMEX-1 expression vector (Promega, Munich, Germany) was followed by recombinant protein production after transformation of BL21(DE)pLysS cells (Novagen, Sigma Aldrich, Munich, Germany) (for details and yields, see Compilation below).

Human galectins obtained by recombinant expression (see Compilation below) were purified by affinity chromatography on lactosylated Sepharose 4B resin as crucial step as routinely applied.

Compilation: expression conditions and yields of recombinant galectins

Protein	Bacterial strain	Expression vector	Expression Temp. °C	IPTG (μM)	Yield (mg/L)
Gal-1	BL21 (DE3) pLysS	pGEMEX-1	37 °C	100 μM	75.20 ± 19.00
Gal-2	BL21 (DE3) pLysS	pGEMEX-1	37 °C	100 μM	10.84 ± 1.18
Gal-4	BL21 (DE3) pLysS	pGEMEX-1	30 °C	75 μM	33.56 ± 23.44
Gal-4P	BL21 (DE3) pLysS	pGEMEX-1	30 °C	75 μM	5.90 ± 1.24
Gal-4V	BL21 (DE3) pLysS	pGEMEX-1	30 °C	75 μM	13.91 ± 6.26
Gal-4N	BL21 (DE3) pLysS	pGEMEX-1	30 °C	75 μM	11.67 ± 7.32
Gal-4C	BL21 (DE3) pLysS	pGEMEX-1	30 °C	75 μM	49.72 ± 32.92

Gal-4CC	BL21 (DE3) pLysS	pGEMEX-1	30 °C	75 µM	0.80 ± 0.35
Gal-8S	BL21 (DE3) pLysS	pGEMEX-1	22 °C	100 µM	24.45 ±3.85
Gal-3—8S—Gal-3	BL21 (DE3) pLysS	pGEMEX-1	22 °C	100 µM	18.78 ± 12.69

Glycoproteins and saccharides for binding assays and assay procedure

Sources and further processing of the glycoproteins for galectin assays have been given previously in detail (Krzeminski et al., 2011). The predominant carbohydrate determinants with affinity to galectins are listed in the footnotes to Table S1 and Table S2. The *Pneumococcus* type 14 polysaccharide was a generous gift from the late Dr. E. A. Kabat (Department of Microbiology, Columbia University, NY, USA). Mono-, di- and oligosaccharides used were obtained from Dextra (Reading, Berkshire, UK) or Sigma (Munich, Germany). In detail, for the assay, the volume of each reagent solution applied to wells of the plate was 50 µL/well, and all incubations, except for coating, were performed at 20 °C. The reagents, if not indicated otherwise, were diluted with tris-buffered saline (TBS; 0.05 M Tris-HCl, 0.15 M NaCl, pH 7.35) containing 0.05 % Tween 20 (TBS-T). TBS-T was used for washing plates between incubation steps.

The surface of 96-well microtiter plate wells (Nunc-Immuno plate, Kamstrupvej, Denmark) was coated with glycoproteins dissolved in 0.05 M sodium carbonate buffer (0.05 M $NaHCO_3$/0.05 M Na_2CO_3, pH 9.6) overnight at 4 °C. After washing the plate, solution with biotinylated hGal-4 (250 ng/well) was added and the plate was then incubated for 30 min. The plates were next carefully washed to remove any free lectin, the ExtrAvidin/alkaline phosphatase solution (diluted 1:10,000; Sigma) was added thereafter to detect the specifically bound Gal-4 by its biotin moieties. After 1 h the plates were washed at least four times to remove free conjugate and then incubated with a solution of *p*-nitrophenyl phosphate (Sigma phosphatase substrate 5 mg tablets) in 0.05 M carbonate buffer, pH 9.6, containing 1 mM $MgCl_2$ (1 tablet/5 mL). The resulting absorbance was read at 405 nm in a microtiter plate reader after 24 h incubation at 20 °C in the dark with the substrate-containing solution. For inhibition studies, serially diluted inhibitor samples were mixed with an equal volume of Gal-4-containing solution. The inhibitory activity was determined from the inhibition curve and is expressed as the amount of inhibitor (ng or nmol per well) giving 50 % inhibition of the control binding.

Array testing for naturally sulfated glycans and their precursors

Probing was performed using biotinylated galectin (50 µg/mL) in a standardized procedure given previously (Blixt et al., 2004; Kutzner et al., 2019). Relative fluorescence units were recorded using the two-step procedure with fluorescent streptavidin, using this optimized protocol.

Crystallization

Crystallization trials were performed at 295 K using the sitting-drop vapor-diffusion method with commercial screening solutions including JBScreen Classic (Jena Bioscience, Jena, Germany) and Wizard Classics I–IV (Emerald Bio, Bainbridge Island, USA) in 96-well sitting-drop plates (Swissci MRC; Molecular Dimensions, Suffolk, England). Drops were set up by mixing equal volumes (0.2 µl) of protein-containing solution and reservoir solution using a Cartesian Honeybee System (Genomic Solutions, Irvine, USA) nano-dispenser robot and equilibrated against 50 µl reservoir solution. Single well-diffracting crystals were obtained in 0.1 M HEPES-NaOH Buffer at pH 7.8 containing 7.5% PEG 4000 and 15% isopropanol.

X-ray Data collection and structure determination

For data collection, crystals were cryo-protected with a cryo-solution containing the reservoir supplemented with 30 % (v/v) ethylene glycol and flash-frozen in liquid nitrogen. X-Ray data collection experiments were performed at the ALBA Synchrotron (Cerdanyola del Vallès, Spain) BL13 XALOC beamline. The data were indexed and integrated, scaled and merged using XDS (Kabsch, 2010). The structure was solved by molecular replacement using the Gal-8 N-terminal CRD structure (PDB: 5GZE) (Si et al., 2016) with Phaser (Adams et al., 2010). The initial model was first refined using Phenix-refine (Adams et al., 2010) and alternating manual building with Coot (Emsley et al., 2010). The final model was obtained by repetitive cycles of refinement; solvent molecules were added automatically and inspected visually for chemically plausible positions. PEG, acetate molecules and the sulfatide ligand, **sulfatide-1**, were added manually. The model was validated and analyzed by MolProbity (Chen et al., 2010). figures illustrating protein structure were drawn with PyMOL (DeLano, 2002). Data collection statistics are listed in Supplementary Table S3.

Supplemental References

Adams, P.D., Afonine, P.V., Bunkoczi, G., Chen, V.B., Davis, I.W., Echols, N., Headd, J.J., Hung, L.W., Kapral, G.J., Grosse-Kunstleve, R.W.*, et al.* (2010). PHENIX: a comprehensive Python-based system for macromolecular structure solution. Acta Crystallogr. *D66*, 213-221.

André, S., Wang, G.N., Gabius, H.-J., and Murphy, P.V. (2014). Combining glycocluster synthesis with protein engineering: an approach to probe into the significance of linker length in a tandem-repeat-type lectin (galectin-4). Carbohydr. Res. *389*, 25-38.

Blixt, O., Head, S., Mondala, T., Scanlan, C., Huflejt, M.E., Alvarez, R., Bryan, M.C., Fazio, F., Calarese, D., Stevens, J.*, et al.* (2004). Printed covalent glycan array for ligand profiling of diverse glycan binding proteins. Proc. Natl. Acad. Sci. USA *101*, 17033-17038.

Bundle, D.R., Ling, C.C., and Zhang, P. Synthetic methods for the large scale production from glucose of analogs of sphingosine, azidosphingosine, ceramides, lactosyl ceramides and glycosyl phytosphingosine. International Patent Classification: C07C 247/08, International Application Number: PCT/CA03/00832, International Publication Number: WO 03/101937 A1, 11.12.2003.

Chen, V.B., Arendall, W.B., Headd, J.J., Keedy, D.A., Immormino, R.M., Kapral, G.J., Murray, L.W., Richardson, J.S., and Richardson, D.C. (2010). MolProbity: all-atom structure validation for macromolecular crystallography. Acta Crystallogr. D*66*, 12-21.

Crich, D., Banerjee, A., Li, W., and Yao, Q. (2005). Improved synthesis of 1-benzenesulfinyl piperidine and analogs for the activation of thioglycosides in conjunction with trifluoromethanesulfonic anhydride. J. Carbohydr. Chem. *24*, 415-424.

DeLano, W. L http://www.pymol.org.

DeLano, W. L. (2002). Pymol: An open-source molecular graphics tool. CCP4 Newsletter On Protein Crystallography, *40*, 82-92

Doyle, L.M., Meany, F.B., and Murphy, P.V. (2019). Lewis acid promoted anomerisation of alkyl O- and S-xylo-, arabino- and fucopyranosides. Carbohydr. Res. *471*, 85-94.

Emsley, P., Lohkamp, B., Scott, W.G., and Cowtan, K. (2010). Features and development of Coot. Acta Crystallog.r *D66*, 486-501.

Furstner, A., Bonnekessel, M., Blank, J.T., Radkowski, K., Seidel, G., Lacombe, F., Gabor, B., and Mynott, R. (2007). Total synthesis of myxovirescin A1. Chem. Eur. J. *13*, 8762-8783.

Kabsch, W. (2010). Xds. Acta Crystallogr. *D66*, 125-132.

Kopitz, J., Bergmann, M., and Gabius, H.-J. (2010). How adhesion/growth-regulatory galectins-1 and -3 attain cell specificity: case study defining their target on neuroblastoma cells (SK-N-MC) and marked affinity regulation by affecting microdomain organization of the membrane. IUBMB Life *62*, 624-628.

Kopitz, J., Ballikaya, S., André, S., and Gabius, H.-J. (2012). Ganglioside GM1/galectin-dependent growth regulation in human neuroblastoma cells: special properties of bivalent galectin-4 and significance of linker length for ligand selection. Neurochem. Res. *37*, 1267-1276.

Krzeminski, M., Singh, T., André, S., Lensch, M., Wu, A.M., Bonvin, A.M.J.J., and Gabius, H.-J. (2011). Human galectin-3 (Mac-2 antigen): defining molecular switches of affinity to natural glycoproteins, structural and dynamic aspects of glycan binding by flexible ligand docking and putative regulatory sequences in the proximal promoter region. Biochim. Biophys. Acta. *1810*, 150-161.

Kutzner, T.J., Gabba, A., FitzGerald, F.G., Shilova, N.V., García Caballero, G., Ludwig, A.-K., Manning, J.C., Knospe, C., Kaltner, H., Sinowatz, F.*, et al.* (2019). How altering the modular architecture affects aspects of lectin activity: case study on human galectin-1. Glycobiology *29*, 593-607.

Ludwig, A.-K., Michalak, M., Xiao, Q., Gilles, U., Medrano, F.J., Ma, H., FitzGerald, F.G., Hasley, W.D., Melendez-Davila, A., Liu, M.*, et al.* (2019). Design-functionality relationships for adhesion/growth-regulatory galectins. Proc. Natl. Acad. Sci. USA *116*, 2837-2842.

Percec, V., Leowanawat, P., Sun, H.J., Kulikov, O., Nusbaum, C.D., Tran, T.M., Bertin, A., Wilson, D.A., Peterca, M., Zhang, S.*, et al.* (2013). Modular synthesis of amphiphilic Janus glycodendrimers and their self-assembly into glycodendrimersomes and other complex architectures with bioactivity to biomedically relevant lectins. J. Am. Chem. Soc. *135*, 9055-9077.

Saal, I., Nagy, N., Lensch, M., Lohr, M., Manning, J.C., Decaestecker, C., André, S., Kiss, R., Salmon, I., and Gabius, H.-J. (2005). Human galectin-2: expression profiling by RT-PCR/immunohistochemistry and its introduction as histochemical tool for ligand localization. Histol. Histopathol. *20*, 1191-1208.

Si, Y., Wang, Y., Gao, J., Song, C., Feng, S., Zhou, Y., Tai, G., and Su, J. (2016). Crystallization of Galectin-8 Linker Reveals Intricate Relationship between the N-terminal Tail and the Linker. Int. J. Mol Sci. *17*, 2088.

Wang, W.W., Angulo-Ibanez, M., Lyu, J., Kurra, Y., Tong, Z., Wu, B., Zhang, L., Sharma, V., Zhou, J., Lin, H.*, et al.* (2019). A Click Chemistry Approach Reveals the Chromatin-Dependent Histone H3K36 Deacylase Nature of SIRT7. J. Am. Chem .Soc. *141*, 2462-2473.

Xiao, Q., Ludwig, A.-K., Romanò, C., Buzzacchera, I., Sherman, S.E., Vetro, M., Vértesy, S., Kaltner, H., Reed, E.H., Möller, M.*, et al.* (2018). Exploring functional pairing between surface glycoconjugates and human galectins using programmable glycodendrimersomes. Proc. Natl. Acad. Sci. USA *115*, E2509-E2518.

Zhang, S., Moussodia, R.-O., Sun, H.J., Leowanawat, P., Muncan, A., Nusbaum, C.D., Chelling, K.M., Heiney, P.A., Klein, M.L., André, S.*, et al.* (2014). Mimicking biological membranes with programmable glycan ligands self-assembled from amphiphilic Janus glycodendrimers. Angew. Chem. Int. Ed. *53*, 10899-10903.

NMR Spectra